國立臺灣大學生命科學院分子與細胞生物學研究所

碩士論文

Institute of Molecular and Cellular Biology

College of Life Science

National Taiwan University

Master Thesis

透過重構 Par 系統研究不對稱細胞分裂

Investigation of asymmetric cell division by reconstituting Par systems

楊承叡

Cheng-Ruei Yang

指導教授：黃筱鈞 博士

Advisor: Hsiao-Chun Huang, Ph.D.

中華民國 111 年 9 月

September 2022

doi:10.6342/NTU202203638

致謝

首先，我想感謝筱鈞老師給我進入實驗室學習的機會，在實驗上提供很多方向讓我發揮，在這兩年的訓練下，老師對於研究的熱忱深深影響了我，讓我對於研究科學的技術以及心態都更加成熟，對於實驗設計的邏輯也更加清晰，未來不論是遇到任何瓶頸有了這兩年的訓練我相信都能夠迎刃而解。謝謝口試委員吳亘承與涂熊林老師，謝謝吳老師在蛋白的實驗上提供了很多實驗的建議，由於細菌的蛋白實驗在我們實驗室是初次建立所以有許多問題需要解決，很感謝吳老師提供了很多實驗可以改良的方向；謝謝涂老師提供一個這麼專業的油滴系統讓我們多了一個研究的面向能夠進行探討，更加豐富我的論文，也謝謝兩位老師在口試的過程中給予我許多寶貴的建議，從兩位老師的提問，我也更加清楚我接下來的實驗該如何更有邏輯的去設計。

謝謝我的家人對我一路以來的栽培，無論做了任何決定都義無反顧地支持我，讓我在求學的路途上可以無後顧之憂。在這段求學的路途上雖然幾乎分隔兩地，但對我的關心與問候從來沒有減少過，中途碰到疫情，幾乎快半年都沒有回家，你們總是擔心我在外面是否安全，也都會寄送一些物資給我，讓我在趕實驗進度時也充滿家人的關心。

特別感謝瑞鐘學長，總是跟我一起待實驗室待到很晚，在疫情封校的兩個月的期間培養出革命情感，甚至在交通不便的狀況下還願意讓家人也順便載我一趟，讓我能夠順利返鄉，也一起幫實驗室解決很多問題，最後在當助理期間甚至還變成我的室友，不知不覺也住了一年多，確診隔離的時候也幫了我很多忙，每天還都幫我送餐，祝福你未來可以達成你的夢想；感謝浩俊學長在實驗上的幫助與教導，很多實驗的原理與背景在你的解說下都淺顯易懂，在你身上我學習到了如何讓實驗設計更有邏輯，蛋白的實驗系統幾乎都是學長一手建立的，也跟我一起解決這系統的許多問題，祝福你出國攻讀博班一切順利。感謝崧丞在處裡行政上的事物都會主動來提醒我，也會時常關心我的實驗進度，祝福你未來一切順利；感

doi:10.6342/NTU202203638

謝耘愷總是會與我分享不同的實驗角度，對於實驗也給予我許多建議，在我確診時也很關心我，幫我處裡好口試的文件與流程，祝福你未來可以順利出國唸書。

感謝正修每次都幫我遠赴中研院涂老師的實驗室操作油滴的實驗，後半段的實驗沒有你真的完成不了，真的幫了我很大的忙，祝福你的實驗能夠越來越順利，未來也順利找到自己想要的工作；謝謝雅筑在自己實驗都忙不過來的情況下還願意協助我的實驗，在我實驗遇到瓶頸時都會主動關心一下，也時常陪我東聊西聊，實驗再怎麼忙碌也要照顧好自己的身體，實驗卡關也不要難過，未來蛋白的實驗系統就交給妳啦，妳真的很優秀，祝福妳未來可以朝向妳的目標大步前進；謝謝佳妏，遇到來自同鄉也念同一所大學的學妹是很難得的緣分，總是跟我還有瑞鐘學長一起做實驗做到很晚，在我忙碌的時候總是會主動幫我買早餐晚餐，甚至在我忙不過來的情況下願意留下來熬夜幫我一起分析數據，假日空閒的時候也都會跟我與瑞鐘學長出門晃晃散心，在我確診時也幫了我很多很多的忙，未來實驗遇到瓶頸也不要灰心，祝福妳可以找到自己的目標一帆風順。

最後我也想感謝我自己在兩年前選擇繼續攻讀碩班，即使在這兩年有點跌跌撞撞，但始終都對自己保持一定的要求，不論實驗或是實驗室的事務上都有盡全力完成，期許未來的自己能時時刻刻保持著初心，利用所學回饋社會。

楊承叡

謹致於 臺灣大學生命科學院 分子與細胞生物學研究所

中華民國 111 年 9 月

doi:10.6342/NTU202203638

摘要

細胞不對稱分裂顯著影響原核和真核生物的分化和功能，會對後代細胞產生不同的命運，對於生物演化的進程再重要不過。在這些生物體中，一個在演化上相對保守的蛋白質家族，Par 蛋白複合物，參與了細胞質內蛋白質的不對稱分佈和不對稱分裂的控制。而其中 PAR-3 本身自我聚合的能力以及 PAR-3 與 PAR-6 兩個蛋白之間的交互作用是造成不對稱性分布的主要因素，這份研究主要是針對 PAR-3 與 PAR-6 進行探討，由於在演化上相當保守，因此我們蒐集了各種不同物種的 PAR-3 與 PAR-6 進行本研究的實驗。我們在這份研究中用了三種不同的系統對 Par 蛋白複合物進行實驗，分別是在大腸桿菌中表現、在油滴的系統中表現以及蛋白質的實驗分析三種不一樣的實驗系統，透過這三種系統的實驗結果讓我們成功地看見 PAR-3 與 PAR-6 兩個蛋白間的交互作用，對於 PAR-3 本身自我聚合的能力則需要再更進一步地探討，在這三種系統的研究成果中有彼此能夠相互印證的地方也有互相不同的地方。三種系統中也都有各自的問題還必須去解決，因此本研究接下來運行的方向可能會朝向將這三個系統去進行整合，我們必須先解決三的系統中各自的問題然後才能對於三個系統的結果進行比較與統整最終才能更進一步清楚地描繪 Par 蛋白複合物整體的運作。

關鍵字:不對稱細胞分裂、大腸桿菌、極化蛋白、蛋白質聚合、油滴系統、液-液相分離

doi:10.6342/NTU202203638

Abstract

Asymmetric cell division significantly affects the differentiation and function of prokaryotes and eukaryotes, and produces different fates for daughter cells, which cannot be more important to the process of biological evolution. In these organisms, an evolutionarily relatively conserved protein family, the Par protein complex, is involved in the asymmetric distribution of proteins within the cytoplasm and the control of asymmetric division. The ability of PAR-3 to self-oligomerize and the interaction to PAR-6 are the key factors causing the asymmetric distribution and division. This study mainly focuses on PAR-3 and PAR-6. For discussion, because they are quite conservative in evolution, we collected PAR-3 and PAR-6 from various species for the this study. We used three different systems to perform experiments on Par protein complex, expression in E. *coli,* droplets, and analysis of proteins. Through these three different systems, the results of the system allow us to successfully find the interaction between the PAR-3 and PAR-6. The ability of PAR-3 to self-aggregate needs to be further explored. The three systems also have their own problems that must be solved, so the direction of this research may be to integrate these three systems. Comparing and integrating the results of the system will eventually lead to a clearer depiction of the overall functioning of the Par protein complex.

doi:10.6342/NTU202203638

Key words: Asymmetric cell division, *Escherichia coli*, PAR complex, Cell free system,

Droplet formation, liquid-liquid phase separation

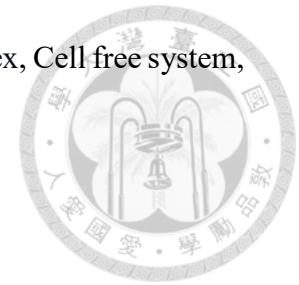

doi:10.6342/NTU202203638

Contents

doi:10.6342/NTU202203638

doi:10.6342/NTU202203638

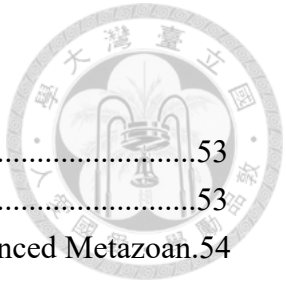

Figure List

doi:10.6342/NTU202203638

Table List

doi:10.6342/NTU202203638

1. Introduction

1.1 Synthetic biology

Synthetic biology integrates engineering concepts and biology science that makes it become an emerging interdisciplinary study program. The origin of synthetic biology is about an idea of *lac* operon (Jacob & Monod, 1961). It described the genetic regulatory mechanisms of synthesis proteins. This idea inspired other designs of the regulatory system (Westerhoff & Palsson, 2004). With the rapid development of technology, it combines a lot of method to design a functional biological system (Abil, Xiong, & Zhao, 2015; Heng & Fussenegger, 2013). One of its concepts is to use mathematical models to combine known proteins or DNA as a component, creating systems that never exist in nature (Benner & Sismour, 2005). It is important for synthetic biology that it can like a group of building blocks, through the bottom-up, creating a functional mechanism we want to do (Purnick & Weiss, 2009). Many synthetic biologists cite Richard Feynman's famous quotations: "What I cannot create I do not understand." The living systems should be re-constructed that make us truly learn the core principles behind the systems of the cells the study of this thesis applies the concept to the polarization of cells and designed base on this advantage.

1.2 Cell polarity

The cell polarity means that there is an asymmetric structure in the cell, which is mainly caused by the uneven accumulation or concentration of substances in some area of the cells. In addition to causing asymmetric cell division, cell polarity also has an important impact

doi:10.6342/NTU202203638

to cell migration, cell shape and structure, and even organization of cellular components. Therefore, the cell types will become more diverse, and each cell will have different functions.

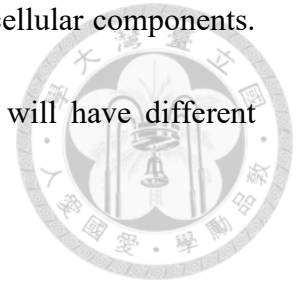

1.3 The important of Asymmetric cell division

Cell differentiation is one of the most processes in the nature. It can be classified into normal cell division (symmetry cell division) and asymmetry cell division. By the process of asymmetric cell division, the daughter cells can present entirely different cellular fate with distinct functions and morphologies (Neumüller & Knoblich, 2009). For example, unlike the normal cell division that generates the same daughter cells, the stem cell will produce differential daughter cells by the unequal distribution of proteins or cytoplasm and development through miosis or mitosis. The mechanism of the asymmetric cell division included four steps, the first is cell polarization, second is polar distribution of cell-fate determinants, the third is polarity axis formation, and the last is cell fate asymmetry segregation (Schweisguth, 2015). In the first step, we can observe there always present a positive feedback on membrane binding protein, and in the next step it will create the protein gradient that make the fate determinants asymmetric distribute into different daughter cells. And then the spindles will prepare for the cell division. Finally, the two daughter cells would be segregated and face different fates. The mechanism of asymmetric splitting has been extensively studied in the past. However, under the complex regulatory network, the traditional top-down approach is limited by many overlapping mechanisms,

doi:10.6342/NTU202203638

which makes it difficult to understand the core principles behind it from the existing complex representations. So, we want to use the constructive approach of synthetic biology, try to build a minimal system from the bottom-up, re-produce the asymmetric division in a single cell, and understand the core system.

1.4 PAR (partitioning defective) complex

The cell fate definition is driven by the segregation of determinants in response to spatial cues. In these organisms, a conserved family of proteins, the Par protein complex, is involved in the asymmetric distribution of cytoplasmic determinants and the control of asymmetric division (Vinot et al., 2005). Par protein complex, including Par-3 (Baz in *Drosophila*), Par-6, and atypical protein kinase (aPKC), are multidomain proteins capable of binding each other and a variety of other cell polarity regulators (Figure 1) (Liu et al., 2020; F. A. Renschler et al., 2018) . The partitioning defective genes were first described in C. *elegans* (Kemphues, Priess, Morton, & Cheng, 1988). In the process of cell fertilization a Par crescent shape is observed on the anterior pole, the mutual inhibition between the anterior (aPKC, Par-3 and Par-6) and posterior (Par-1 and Par-2) poles leads to different fates of daughter cells (Hwang & Rose, 2010). For another representative model is the cell division process of *Drosophila* in neuroblasts, at the beginning of mitosis, the evenly distributed Baz/Par6/aPKC protein gradually concentrates and forms a crescent shape in the apical cortex, while the cell fate determinants and their adaptor proteins,

doi:10.6342/NTU202203638

partners of the Numb/Pon complex and the Prospero/Miranda complex form a crescent in the basal cortex, thereby establishing apical-basal polarity (Ikeshima-Kataoka, Skeath, Nabeshima, Doe, & Matsuzaki, 1997; Petronczki & Knoblich, 2001).

1.5 The structural domains of Par-3 family

Par-3 is a scaffold protein for the complex. The family of polarity determinants is highly conserved in metazoans. For example, *C. elegans* PAR-3, *Drosophila* Bazooka (Baz), human Par-3 (PARD3), are all included in the family (Thompson, 2022). Par-3 has three PDZ (PSD-95, DLG, and ZO-1) domains that mediate protein-protein interactions. PDZ domains can act singly or synergistically to bind the C-termini of interacting proteins. Sequence comparisons between Baz, human and *C. elegans* Par-3 shows divergence in the peptide-binding area of PDZ1 and greater conservation for of the others(Yu et al., 2014). Par-3 thus has the potential to recruit two Par-6 proteins at the same time because of a structural analysis by x-ray crystallography and NMR spectroscopy reported that both the PDZ1 and PDZ3 domains engaged interaction with the PDZ domain–binding motif of Par-6 (Fabian A. Renschler et al., 2018). It may help the polarity proteins create networks through multivalent PDZ domain interactions. And about the second PDZ domain, it may mediate membrane interaction. In addition to the common set of proteins, phosphoinositides (PIPs) are also known to play critical roles in cell polarity with Par-3. The second PDZ domain of Par-3 binds to phosphatidylinositol (PI) lipid membranes with

doi:10.6342/NTU202203638

high affinity (Wu et al., 2007). Despite the above understanding, the mechanism by which Par-3 interacts with PIP2 on the membrane and whether the phenomenon of Par-3 forming phase separation really plays any decisive role in the asymmetric split still needs further discussion. In addition to three PDZ domains, Par-3 also contains a conserved N-terminal oligomerization domain (NTD) that is essential for proper subapical membrane localization and consequently the functions of Par-3 (Feng, Wu, Chan, & Zhang, 2007). And because of the NTD domain of Par-3, it can promote oligomerization and make Par-3 undergoes phase separation (Liu et al., 2020). Besides, Par-6 can use C-terminal tail binding to the of Par3 PDZ3 and promote the phenomenon of phase separation in Par-3. The study demonstrates that the NTD-mediated membrane localization of Par-3 is attributed to its oligomerization capacity. Par-3 NTD is likely to help the assembly of PAR complex.

1.6 Liquid–Liquid phase separation (LLPS)

Liquid-liquid phase separation also known as biomolecular condensates or droplets is believed to be important in many aspects of biology. It represents an ubiquitous phenomenon in the formation of membrane less organelles in eukaryotic cells (Wang et al., 2021). For example, P granules are aggregates non-membrane-bound RNA protein compartments involved in germline development in *C. elegans*. P granules are distributed asymmetrically during development. When embryos are in a single-cell state, they are evenly distributed throughout the cytoplasm, but as the single cell begins to division, P

doi:10.6342/NTU202203638

granules gradually converge toward the back of the cell and these circular droplets are formed at the boundary, fusing into larger droplets after contacting each other. This results in asymmetric cell division (Saha et al., 2016). Another important study describe the condensation of the Par complex during cell polarization is driven by LLPS.

1.7 Asymmetric cell division in non-bilateral animals

Par complex considered to be a metazoan innovation because of the conserved in the genome of sequenced metazoan. Asymmetric cell division has been discussed in many literatures in the past and the role of the Par complex has been extensively studied in Metazoan, but the function in epithelial and early embryogenesis has only been described in some bilateral animals. However, there were no relevant description could be found in the literature in non-bilateral animals (Figure 3). To reconstructing the evolutionary of Par complex, we need to study non-bilateral animals (Salinas-Saavedra, Stephenson, Dunn, & Martindale, 2015). The *Nematostella vectensis* is a kind of sea anemone represent one of cnidarian and non-bilaterians. The par proteins in N. *vectensis* are distributed throughout in early embryos and no polarity happened at this stage. However, these proteins would distributed asymmetrically when embryos start to form epithelium. In addition to cnidarian, another animal porifera also can help us understand the origin of Par complex. The *Amphimedon queenslandica* is a kind of sponge represent of porifera (Belahbib et al., 2018; Fahey & Degnan, 2010). Compare with bilaterian, the proteins in *Amphimedon* possess a

doi:10.6342/NTU202203638

complement that act to establish cellular apical–basal polarity. There are many genes maintain conserved sequences between the sponge and metazoan. So, these mechanisms and complexes may operate in a conserved manner in *Amphimedon*. All these data strongly suggest that aPKC, Par-3 and Par-6 have co-evolved from a functional metazoan ancestral complex (Belahbib et al., 2018).

1.8 Asymmetric cell division in *E. coli*

E. *coli* performs binary cell division in the cell cycle, so many scientists use this feature to test the asymmetric cell division in it. One of the asymmetric cell division models in E. *coli* is built by polar organizing protein Z (PopZ) (Mushnikov, Fomicheva, Gomelsky, & Bowman, 2019). PopZ is an upstream and polarity proteins can self-organize into large oligomer through its C terminal oligomerization domain. Previously, in our laboratory we reconstruct asymmetric cell division with PopZ in E. *coli* and successfully make the gene expression asymmetrically. Besides, we also used PodJ as the second pole to reconstruct the two-pole system for asymmetric division in E. *coli.*

doi:10.6342/NTU202203638

1.9 Aim

In this study, we want to use *E. coli* serve as a platform to create Par protein complex asymmetric cell division. So, we search many Par protein in different species. First, we referred to the article (Liu et al., 2020) (Figure 2) and synthesized two gene fragments, Par-3N (rat, *E. coli* codon optimized) and Par-6β (mouse, *E. coli* codon optimized), by gene synthesis. In this article, we can know that the par-3N can form puncta undergoes LLPS by its oligomerization and when interact with Par-6β, can promote this phenomenon. Then, we get a list of Par protein in different species from Fumio Motegi. (Table 1.) In addition to *E. coli*, we also want to try to establish the phenomenon of cell polarity in the cell-free systems such as droplet system. The reason we want to use this system is described below. First, if we need to explore at a larger scale of asymmetric division, the oligomerization and limited diffusion of PopZ and DivIVA may not sufficient to drive asymmetric division, and phase separation may be necessary to establish intracellular asymmetry at larger scales. Then, compared with *E. coli*, droplet has a simpler environment. For example, if we want to express in *E. coli*, we must find a protein that is orthogonal to *E. coli*. However, that would not be a problem in the droplet. A technique based on microfluidic synthetic droplets has recently emerged, which allows for better control over size and other functions. Therefore, we can focus on the protein. Because of that, we want to performance the reconstitution of polarity protein network in droplets. Besides, we also run proteins gel in this study. We want to use this way to simply looking at the interactions between the

doi:10.6342/NTU202203638

proteins (Par-3 and Par-6). So, we use Immunoprecipitation for the purification of a proteins and run SDS PAGE and NATIVE GEL, using the Western blotting to probe the proteins in the aspect of this study. Finally, we want to through these three different aspects to explore and discuss the interactions and some phenomenon between the Par complex proteins.

Table 1. Par complex in different species from Fumio Motegi.

C.*elegans* cDNAs (C. *elegans* codon)	**Par-3** **Par-6**
C.*elegans* cDNA (Yeast codon optimized)	**Par-6**
Par-3 homologues	**Sponge (E. *coli* codon optimized)** **Anemone (Yeast codon optimized)** **Fly codon** **Mouse codon (150 kDa isoform)** **Mouse codon (100 kDa isoform)** **Human codon**

<Note >

(1) The synthesized proteins, Par-3N (rat) and Par-6β (mouse) were *E. coli* codon optimized.

(2) The fluorescent protein (sfGFP, mRFP, mCherry) and protein tag (His tag, FLAG tag) used in this study were E. *coli* codon.

doi:10.6342/NTU202203638

2 Materials and methods

The experiment of E. *coli*

2.1 Bacteria strains

In our laboratory, we display lots of plasmid to express in *E. coli*. The strain of DH5α is a versatile strain used for general cloning and because of the mutation *rec*A1 gene, increased the insert stability and available in a wide variety of transformation efficiencies, so the strain is the most popular *E. coli* strain for our cloning application.

In this study, we also use BLR (DE3) strain. The BLR strain is a *rec*A- derivative of BL21 strain to improve its plasmid yields; DE3 means that the host is a lysogen of λDE3, because of that it has a chromosomal copy of the T7 RNA polymerase gene under the lacUV5 promoter control. Therefore, this strain is suitable for production of protein from target genes in vectors by IPTG induction (Figure 4).

2.2 The culture Medium

Luria-Bertani (LB) liquid medium is a kind of commonly to culture *E. coli*. So, in our laboratory, we use this medium to help us culture bacteria and do different tests. The preparation of Luria-Bertani liquid medium is shown in Table 2.1.

Table 2.1 Luria-Bertani (LB) liquid medium.

Component	amount(g)
Tryptone	10g
NaCl	10g
Yeast Extract	5g
Total distillation water(L)	1 liter

For our experiment we also need to select a single colony. Therefore, solid LB medium can help us separate the colony. The preparation of solid LB medium was shown in Table 2.2.

doi:10.6342/NTU202203638

Table 2.2 Luria-Bertani (LB) agar plate.

Component	amount
Tryptone	10g
NaCl	10g
Yeast Extract	5g
Agar	15g
Total distillation water	1 liter

2.3 Concentration of antibiotic

Antibiotics had a range of function that could stop bacteria contamination, and prevented bacterial growth. In our cloning experiment, when we completed the step of ligation, the product of ligation had to be transformed to competent cell and grew on LB agar plate with specific antibiotic. If the vector and insert successfully connected, the final plasmid would have a backbone with antibiotic resistance gene. Thereby, it could be screened out through LB agar with antibiotics, and picked out colonies. There were three kinds of antibiotics that we frequently used. The concentration we use were shown in Table 2.3.

Table 2.3 The amount of antibiotic.

Antibiotics	Solvent	Concentration of usage (μg/ml)	Concentration of stock (mg/ml)
Chloramphenicol	100%EtOH	35	35
Ampicillin	Distillation water	100	100
Kanamycin	Distillation water	50	50

2.4 Bacteria plasmid extraction

After separate and select the single colony, we need to purified bacteria plasmid DNA. We use Mini Plus Plasmid DNA Extraction kit by VIOGENE. It can help us extract plasmid DNA from bacteria fast and efficiency without chloroform or phenol extraction. The

doi:10.6342/NTU202203638

protocol of this kit is following.

1. Following bacteria culture, set a density of the bacteria broth to OD_{600} of 2.
2. Pour the bacteria broth into a 2ml sterile Eppendorf and centrifuge for 1 minute (13,500rpm) and collect the bacteria pellet remove the supernatant.
3. Repeat step 2 until collecting all pellet.
4. Resuspend the pellet in 200μl MX1 Buffer (with RNase) vortex completely.
5. Add 250μl MX2 Buffer and invert the Eppendorf about 30 seconds until the mixture becoming clear, waiting in room temperature for 3 minutes.
6. Add 350μl MX3 Buffer, and gently mix well, then centrifuge at 13,000 rpm for 10 minutes.
7. Transfer the supernatant from Eppendorf into Mini plus column. After that, centrifuge at 9,000 rpm for 1 minute, and discard the flow-through.
8. Add 500μl of WN Buffer by centrifuging at 9,000 rpm for 1 minute.
9. After discarding the flow-through, add 700μl WS Buffer and centrifuge at 9,000 rpm for 1 minute, and discard the flow-through.
10. Centrifuge at 13,000 rpm for 3 minutes to remove residual liquid.
11. Place the column to a new sterile 1.5 ml Eppendorf, and then place into Dry-bath for 3 minutes
12. Add 30μl distillation water into the membrane.
13. Stand at room temperature for 3 minutes, and then centrifuge at 13,000 rpm for 2 minutes.
14. Finally, collect plasmid DNA, store at 4°C or -20°C.

doi:10.6342/NTU202203638

2.5 Gel extraction for DNA fragment

The tool is the kit of Gel Advanced Gel Extraction Miniprep System from VIOGENE to help us extract DNA fragment which was digested by restriction enzyme and separated by DNA electrophoresis with TAE gel.

1. After cutting required DNA fragment form agarose gel, add 500μl GEX Buffer and put the gel into a 2.0 ml sterile Eppendorf.
2. Incubate the tube at Dry-bath 60°C about 10 minutes until the gel completely melted.
3. Put the tube in room temperature to cool down slowly.
4. Transfer the dissolved gel to GP™ column, and centrifuge at 9,000 rpm for 1 minute, and discard the flow-through.
5. Add 500μl WN Buffer into GP™ column, centrifuge at 9,000 rpm for 1 minute, discard the flow-through.
6. Add 500μl WS Buffer into GP™ column, centrifuge at 9,000 rpm for 1 minute, discard the flow-through.
7. Centrifuge the column at 13,000 rpm for 3 minutes to remove residual liquid.
8. Place the column to a new 1.5 ml Eppendorf, then Dry-bath for 5 minutes to increase the purity of DNA fragment.
9. Add 30μl distillation water onto the membrane, and stand at room temperature for 3 minutes.
10. Centrifuge at 13,000 rpm for 3 minutes, then collect the eluted product used for ligation or storing at 4°C or -20°C.

2.6 Primer design

In our laboratory, we use SnapGene to design the primers. The primer Tm value and annealing temperature are checked with NEB Tm Calculator (https://tmcalculator.neb.com/). And we also use Oligo v7 to help us predict the Tm value of hairpin loop structures in each primer.

doi:10.6342/NTU202203638

2.7 Polymerase chain reaction (PCR)

PCR is a widely method of molecular biology to replicate and amplify target DNA fragments in vitro. The enzyme in our laboratory are Q5® High-Fidelity DNA Polymerase and Phusion High-Fidelity DNA polymerase from New England BioLabs (NEB). These enzymes provide higher fidelity amplification than *Taq* polymerase. The configuration of PCR yield is 50μl and the proportion reagent of PCR is listed in Table 2.4 and 2.5 and run with the thermocycling condition listed in Table 2.6.

Table 2.4 Reagent of Q5®PCR

Component	Amount (μl)	Concentration
DNA Template	1	1 ng/μl
5X Q5 Reaction Buffer	10	1X
5X GC Enhancer Buffer	10	1X
Forward DNA primer	2.5	0.5μM
Reverse DNA primer	2.5	0.5μM
dNTPs	1	200μM
Q5 polymerase enzyme	0.5	0.02 units/μl
Distillation water	22.5	---

Table 2.5 Reagent of Phusion PCR

Component	Amount (μl)	Concentration
DNA Template	1	1 ng/μl
5X Phusion GC Buffer	10	1X
Forward DNA primer	2.5	0.5μM
Reverse DNA primer	2.5	0.5μM
dNTPs	1	200μM
Q5 polymerase enzyme	0.5	0.02 units/μl
Distillation water	32.5	---

doi:10.6342/NTU202203638

Table 2.6 Thermocycling condition

Step	Temperature	Time
Initial denaturation	98℃	30s
Denaturation	98℃	10s
Annealing	Perdition by NEB Tm calculator	30s
Extension	72℃	1000 bp/30s
Go back to denaturation step for 35 cycles		
Last extension	72℃	2mins
Hold on	12℃	---

doi:10.6342/NTU202203638

2.8 PCR product clean up

There are many buffer or enzyme in the mixture after we performed PCR reaction. To remove these residues, we use the kit of PCR Advance PCR clean up system from VIOGENE to purify the PCR products.

1. After completing the step of PCR, the PCR product and 500μl of PX Buffer were added to a new sterile 1.5 ml Eppendorf, and mix them.
2. After mixing well, add the mixture product onto a GP^{TM} column and centrifuge at 9,000 rpm for 1minute, and discard the flow-through.
3. After discarding the flow- through, add 500μl of WN Buffer to wash the column, and centrifuge at 9,000 rpm for 1 minute.
4. After discarding the flow- through, add 500μl of WS Buffer to wash the column, and centrifuge at 9,000 rpm for 1 minute.
5. After discarding the flow- through, remove the residual liquid by centrifuging the column at 13,000 rpm for 3 minutes.
6. Replace the column with a new sterile 1.5 ml Eppendorf, then place into Dry-bath for 3 minutes to increase the purity of DNA fragment.
7. Add 30μl of distillation water onto the membrane, and stand at room temperature for 3 minutes.
8. Centrifuge at 13,000 rpm for 2 minutes, then collect the eluted DNA fragment used to restriction enzyme digesting or storing at 4°C or -20°C.

2.9 Circular polymerase extension cloning (CPEC)

Circular polymerase extension cloning is one of the strategies to create different short DNA fragments. The process of CPEC don't need restriction enzyme different from BioBrick. This method base on polymerase to extend target DNA sequences, we can design overlapping

doi:10.6342/NTU202203638

sequence between insert and vector DNA fragments. Via specific primer PCR process, the insert and vector will be combined by overlapping site.

2.10 Restriction enzyme digestion

The restriction enzymes used in this study were produced from New England BioLabs (NEB), and the mixture were incubated at 37℃ for 3 hours.

Table 2.7 restriction enzymes preparation.

Component	Amount
DNA	＜1000 (ng/μl)
CutSmart^{TM} buffer	3μl
restriction enzyme	1μl for each
Distillation water	Add to 30μl

2.11 Agarose electrophoresis

After plasmid digesting, we need to separate the specific length of DNA fragment. We use agarose gel electrophoresis to separate DNA fragments and check the length of plasmid or PCR product. Dissolving 1% agarose into 1X Tris acetate EDTA buffer (TAE buffer) and adding SafetyView dye. The sample and 6X loading dye would be mixed before loading into the gel. The marker 1K to 100bp can help us identify the length of samples. The condition of electrophoresis running is 110 voltage for 30 minutes in 1X TAE buffer. After that, we check the length under blue light lighting.

doi:10.6342/NTU202203638

2.12 BioBrick Assembly

One of the most important of cloning is that we need to make one gene as an insert fragment add into a vector gene. BioBrick assembly is a gene assembly way based on enzyme digestion and DNA ligation. It is very common to use this method combining multiple fragment including target gene into a single plasmid.

We simplify the original process in our system, we only use four restriction enzymes, EcoRI, XbaI, SpeI, and PstI. The first key makes the system work is that the cutting sites of XbaI and SpeI leave the same overhang sequence, means that can form a "scar" (compatible ends) and never be recognized by XbaI and SpeI next time. Second, the sites of EcoRI and PstI cutting can generate "sticky end", so the T4 DNA ligase can combine the sites.

2.13 Ligation

After restriction enzymes digesting, the two DNA fragments can connect by using T4 DNA ligase from New England BioLabs (NEB). The volume ratio between insert and vector is always 3:1 in our lab. The mixture contains insert and vector DNA, T4 ligase buffer and T4 ligase. The condition of the DNA ligation mixture was shown in Table 2.8. After that, put the DNA ligation mixture at 16 °C for 14 hours.

Table 2.8 Reaction system of DNA ligation.

Component	Amount(μl)
10X T4 DNA ligase reaction buffer	1
T4 DNA ligase	0.5
Insert and Vector DNA	8.5

doi:10.6342/NTU202203638

2.14 Gibson Assembly

The Gibson Assembly is a gene assembly method. The only condition that this method need is the binding sites between the fragments should 20 bp overlapping at least. Because of that this method don't need any restriction enzyme and could combine up to 15 fragments in a single reaction with the seamless ligation. We use NEBulider HiFi DNA Master Mix from New England BioLabs (NEB) in this method. There are three different enzymes in the reaction mixture would combine the fragments in 4 steps. First, 5' exonuclease cuts back DNA from 5'end and fragments would be annealing in 3'overhang of overlapping region then DNA polymerase removes the gap in the fragments, and DNA ligase connect the nicks. The mixtures contain 2.5μl (insert and vector with 2:1 ratio) and 2.5μl NEBulider HiFi DNA Master Mix incubate at 50℃ for 15 minutes.

2.15 Chemical plasmid transformation

In this study, we used DH5α and BLR(DE3) as competent cell. Heat shock to transform our target plasmid into competent cell.

1. Mix plasmid and competent cell with the ratio of 1:5 by tapping.
2. Place the mixture on ice for 30 minutes.
3. Incubate the mixture on the water bath at 42°C for 45 seconds.
4. Place the mixture on ice for 5 minutes.
5. Transfer the mixture into 1 ml LB broth, and incubate at 37°C for 45 minutes to 1 hour.
6. Spread the mixture on the LB agar plate with target antibiotic.
7. Incubate the LB agar plate at 37°C overnight.

doi:10.6342/NTU202203638

2.16 Fluorescent Microscopy

In our laboratory, we use Zeiss AxioObserver Z1 inverted microscope to capture all fluorescence microscope images. Because of E. coli is very small and high mobility, it is very difficult to capture with 100X oil objective. So, we put water agarose on the top of the bacteria to inhibit its mobility. And to place the water agarose pad, we use the ibidi, a chambered slide with 8 wells for microscopy. The following is the protocol of the preparation.

1. Add the 1% water agarose into the space between two slides.
2. After it turn into solid, cutting the gel into suitable size and add 2μl germ on the gel.
3. Flipping the gel into an ibidi chamber slide.
4. Capture the fluorescent images on Zeiss AxioObserver Z1.

2.17 The method of statistical analysis

We use Oufti (https://oufti.org/) program to abstain the cells fluorescence signals, The program is an open-source software package designed for analysis of microscopy data to extract and measure the fluorescence intensity of cell individually (Paintdakhi et al., 2016). This program divides the cell into 100 areas along with the axis. The data would be input to our python code for analysis the cell polarity metrics and Person correlations. Both the values of cell polarity metrics and Person correlations would be drawn into figures with Prism9.0. There is an analysis method in our python code named Otsu's thresholding method (Ting & Chengyuan; Xu, Xu, Jin, & Song, 2011). By this method, we can only reserve the cell that the sum of 1/3 cell length.

2.18 Primer List for sequencing

To make sure the DNA sequence of plasmid parts, we send the sequencing samples and related primers which directed the site of sequencing beginning. The sequencing primers that we used are listed in Table 2.9.

doi:10.6342/NTU202203638

Table 2.9 Primer list

Primer name	Sequence (5’ to 3’)
VF2	TGCCACCTGACGTCTAAGAA
VR	ATTACCGCCTTTGAGTGAGC
CmR(F)	GCCATCACAAACGGC
CmR(R)	CGCAAGGCGACAAGG
pLux promoter	CTTTCTGCGTTTATATACTA
LuxR	GTTATTAATTTTTAAAGTATG
pTac promoter	GGAACGATCGTTGGCTGTG
lacI	ATTCACCACCCTGAATTGACTCT
mRFP N terminal forward	GCCCATAACATCACC
mRFP N terminal backward	GCTTCCTCCGAAGACGTTAT
mRFP C terminal forward	GTCGTCACTCCACCGGTGCT
mRFP C terminal backward	CATCACCTCCCACAACGAAG
sfGFP N terminal forward	GCCCATTAACATCACC
sfGFP N terminal backward	AGCAAAGGAGAAGAACTTTT
sfGFP C terminal forward	GGCATGGATGAGCTCTACAA
sfGFP C terminal backward	GACCACATGGTCCTTCTTG
mCherry N terminal forward	TCCTCGCCCTTGCTCACCAT
mCherry N terminal backward	ATGGTGAGCAAGGGC
mCherry C terminal forward	CTTGTACAGCTCGTCCATG
mCherry C terminal backward	GCATGGACGAGCTGTACAAG

Primer name	Sequence (5’ to 3’)
Worm par3 (T)	ATGTCGGCTTCATCCACGTC
Worm par3 (B)	CTAGTACTGGGGAAAACGATG
Sponge par3 (T)	ATGTCTAAGCCAAGATTGAGA
Sponge par3 (B)	TAATGCTCTAGTGTTATGAGAAG
Anemone par3 (T)	ATGAAGAAAAATAAGACTTTCGATTTCAAC
Anemone par3 (B)	AACTCTTGTTGGTTGAGAAACAATA
Baz par3 (T)	ATGAAGGTCACCGTCTGCTT
Baz par3 (B)	TCACACCTTGGAGGCGTG
Mouse par3 150kDa (T)	ATGAAAGTGACCGTGTGCTT
Mouse par3 150kDa (B)	TCAGGAGTAGAAGGGCCG
Mouse par3 100kDa (T)	ATGCCTCTTCATGTCCGC
Mouse par3 100kDa (B)	TCATCTCTTCTCCGGCTTCA
Human par3 (T)	ATGAAAGTGACCGTGTGCTT
Human par3 (B)	TCAGGAATAGAAGGGCCTCC

doi:10.6342/NTU202203638

Primer name	Sequence (5’ to 3’)
Worm par6 (T)	ATGTCCTACAACGGCTCCTA
Worm par6 (B)	TCAGTCCTCTCCACTGTCC
Yeast codon optimized par6 (T)	ATGTCCTACAACGGTTCCTA
Yeast codon optimized par6 (B)	GTCTTCACCAGAATCGGAGT

The experiment of Protein

2.19 Sample lysis

Centrifuge the bacteria LB broth at 14,800 rpm and use 0.9% NaCl solution wash 2 times and discard the supernatant. Dissolve the pellet with LE buffer in ratio of 10μl /mg and add 1mM PMSF. The sonic probe operates at >60kHz. Turn on the sonic probe for 3 seconds and pause 5 seconds per around and run 10 minutes. After lysis spin down the cell debris at 14,800 rpm at 4°C for 15 min. Move the supernatant to a new tube and keep cold. Total cell lysates were extracted with LE buffer and quantified with Bradford protein assay (Bio-rad).

2.20 Immunoprecipitation (IP)

Immunoprecipitation is a method that enables the purification of a protein. In this study, we used the Ni-charged Magbeads. The Ni-Charged MagBeads have a binding capacity of 6xHis-tagged protein isolation & pulldown (figure 5).

1. Add 20μl beads solution into a new sterile 1.5 ml Eppendorf and separate the beads from solution by magnetic forces, discard the supernatant.
2. Add 200μl LE buffer completely mixes with beads and separate the beads from solution by magnetic forces discard the supernatant. Repeat again.
3. Add 200μl cell lysate completely mixes with beads and incubates on ice shaking for 1 hours
4. Separate the beads from solution by magnetic forces and discard the supernatant.
5. Add 200μl wash buffer completely mixes and discard the supernatant. Repeat 4 times.

doi:10.6342/NTU202203638

6. Add 100µl Elution buffer 1 completely mixes with beads and reserve supernatant by magnetic forces.
7. Add 100µl Elution buffer 2 completely mixes with beads and reserve supernatant by magnetic forces.
8. Add 100µl Elution buffer 3 completely mixes with beads and reserve supernatant by magnetic forces.
9. Add 100µl Elution buffer 4 completely mixes with beads and reserve supernatant by magnetic forces.

2.21 Western blotting analysis

Sample preparation

The sample and 5X loading dye would be mixed and incubated at 90℃for 10 minutes in PCR machine before loading into the gel.

.

Loading and running the gel

The molecular weight protein standard marker can help us identify the molecular weight of samples (in kDa). The condition of SDS PAGE (stacking gel) electrophoresis running is 70 voltage for 30 minutes in running buffer. The condition of SDS PAGE (main gel) electrophoresis running is 110 voltage for 1 hour in running buffer. The condition of NATIVE GEL electrophoresis running is 100 voltage for more than 1 hours in running buffer without SDS .

Protein fast stain

We use Imperial^{TM} protein stain (Thermo) to help us check the protein bands.

1. Place the protein gel in a clean box and wash 3 times for 5 minutes each with water.

doi:10.6342/NTU202203638

2. Add 15ml Imperial™ protein stain into the box and stain for 1 hour with gentle shaking.
3. Place the protein gel in water for 2 hours with gentle shaking and change the wash buffer frequently.

Transfer the protein gel to membrane

After running the SDS PAGE or Native gel electrophoresis. The protein gels were transferred onto immobilon-P PVDF membrane.

1. Incubate the protein gels in the transfer buffer
2. Activate PVDF with methanol for one minute and incubate with transfer buffer before preparing the stack.
3. Prepare the stack as the Figure 6.
4. Put the stack in the transfer tank and fill up the tank with transfer buffer and put a stirrer in the tank.
5. Put the transfer tank in the bucket and fill the ice bucket with ice.
6. Place the system on magnetic stirrer and make sure the stirrer can work.
7. Star transfer for one hour with 100 voltage at 4°C.
8. After the transfer, wash the membrane with distillation water and check the transfer of proteins to the membrane using Ponceau S staining before the blocking step.
9. Afterwards, membranes were rinsed with distillation water and make sure no Ponceau S residue then blocked with Gelatin net for 1 hour in room temperature or overnight in 4℃.

Ponceau S stain

Ponceau S is a reversible stain method used for detection of proteins on PVDF membranes.

1. Rinse the PVDF membrane in methanol.
2. Rinse in distillation water.
3. Incubate in the stain for 10 minutes at room temperature.

doi:10.6342/NTU202203638

4. Check the proteins bands
5. Rinse in distillation water until the background is completely removed.

Antibody staining

1. Block the membrane with gelatin net for one hour at room temperature or overnight at 4°C.
2. Incubate the membrane with appropriate dilutions (five or ten thousand) of anti-His tag or anti-FLAG tag primary antibody in gelatin net for one hour at room temperature or overnight at 4°C.
3. After the antibodies binding, wash the PVDF membrane in three times of PBST for 10 min each.
4. Incubate the PVDF membrane with the appropriate dilution (five or ten thousand) of corresponding secondary antibodies in blocking buffer at room temperature for one hour. The corresponding secondary antibodies conjugated horseradish peroxidase (HRP) that can visualize the Immunoreactive proteins.
5. After the antibodies binding, wash the PVDF membrane in three washes of PBST for 10 min each.
6. Using enhanced chemiluminescence (ECL) detection system. Mix the reagent A and reagent B with the dilution ratio one to one. Add the mix reagent onto the sample PVDF membrane. Remove excess reagent and cover the membrane in transparent plastic wrap.
7. Using the chemiluminescence imaging System to acquire image.

Stripping

The stripping buffer can remove the antibodies from Western blot effectively that the stripped membrane can re-probing with different antibodies.

doi:10.6342/NTU202203638

1. Pour stripping buffer 15ml to a clean container and put the PVDF membrane in it.
2. Incubate the membrane in the buffer for 10 minutes at room temperature with strong agitation.
3. Wash 2 times for 5 minutes in PBST at room temperature using a lot of volumes.
4. Block the PVDF membrane to reuse.

Solutions and reagents:

Table 2.10. Solution for preparing LE buffer

Solution components	Component volumes
NaH_2PO_4	50mM
NaCl	300mM

✓ Adjust the pH value to 7.4.

Table 2.11. Solution for preparing wash buffer

Solution components	Component volumes
NaH_2PO_4	10mM
NaCl	300mM
imidazole	10mM

✓ Adjust the pH value to 7.4.

Table 2.12. Solution for preparing Elution buffer 1

Solution components	Component volumes
NaH_2PO_4	10mM
NaCl	300mM
imidazole	25mM

✓ Adjust the pH value to 7.4.

✓ The Elution buffer 2-4 is different in the value of imidazole. The volumes in 2-fold increments

doi:10.6342/NTU202203638

Table 2.13. Solution for preparing 10X running buffer

Solution components	Component volumes (1L)
Tris (base)	250mM
Glycine	1920mM
SDS	10g

✓ Dissolve in 1L distilled water and dilute to 1X before use.

✓ The pH of the buffer should be 8.3 and no pH adjustment is required.

Table 2.14. Solution for preparing 10X transfer buffer

Solution components	Component volumes (1L)
Tris (base)	250mM
Glycine	1920mM

✓ Dissolve in 1L distilled water.

✓ Add methanol with 1:2 ratio and dilute to 1X before use.

Table 2.15 Solution for preparing Gelatin net (blocking buffer)

Solution components	Component volumes (1L)
Gelatin	2.5g
NaCl	8.75g
Tris (base)	6.05g
EEDTA · 2Na	1.8g
Tween 20	0.5ml

✓ Dissolve in 800ml distilled water and adjust pH value to 8.0.

✓ Bring volume up to 1L with distilled water.

doi:10.6342/NTU202203638

Table 2.16. Solution for preparing 1X PBST

Solution components	Component volumes (1L)
KH_2PO_4	1.8mM
Na_2HPO_4	10mM
KCl	2.7mM
NaCl	137mM
Tween 20®	0.1%

✓ Dissolve in 800ml distilled water and adjust pH value with HCl to 7.4-7.6.

✓ Bring volume up to 1L with distilled water.

Table 2.17. Solution for preparing stripping buffer

Solution components	Component volumes (1L)
Glycine	15g
SDS	1g
Tween 20®	10ml

✓ Dissolve in 800ml distilled water and adjust pH value with HCl to 2.2.

✓ Bring volume up to 1L with distilled water.

Table 2.18. Solution for preparing Ponceau S

Solution components	Component volumes (1L)
Ponceau S	1g
Acetic acid	50ml

✓ Dissolve in 1L distilled water

doi:10.6342/NTU202203638

SDS PAGE

Table 2.19. Solution for preparing 8% SDS PAGE (MAIN GEL)

Solution components	Component volumes (ml)
distillation water	2.3
30% acrylamide mix	1.3
1.5 M Tris (ph 8.8)	1.3
10% SDS	0.05
10% ammonium persulfate	0.05
TEMED	0.003

Table 2.20. Solution for preparing SDS PAGE (STACKING GEL)

Solution components	Component volumes (ml)
distillation water	0.55
30% acrylamide mix	0.17
0.5 M Tris (ph 8.8)	0.26
10% SDS	0.01
10% ammonium persulfate	0.01
TEMED	0.001

doi:10.6342/NTU202203638

Native GEL PAGE

Table 2.21. Solution for preparing 10% NATIVE GEL (MAIN GEL)

Solution components	Component volumes (ml)
distillation water	4.11
30% Bis-Acrylamide	3.33
1.5 M Tris (pH 8.8)	2.5
10% ammonium persulfate	0.05
TEMED	0.005

Table 2.22. Solution for preparing NATIVE GEL (STACKING GEL)

Solution components	Component volumes (ml)
distillation water	6.2
30% Bis-Acrylamide	1.33
0.5 M Tris (pH 6.8)	2.5
10% ammonium persulfate	0.05
TEMED	0.005

doi:10.6342/NTU202203638

The experiment of Droplet

2.22 In Vitro Transcription/Translation System (IVTT)

For droplets experiments, we need to use the in vitro transcription and translation kit to help us produce target proteins in the droplets. The kit contains E. *coli* RNA polymerase.

1. Place the solutions I II and III on ice.
2. Prepare reaction mixtures in either nuclease-free 0.5 ml Eppendorf tubes.
3. Add template DNA.
4. Incubate samples at 37°C for 3 hours to allow for transcription and translation.
5. Stop the reaction on ice.

Table 2.23. Solution for preparing IVTT kit

Solution components	Component volumes (μl)
distillation water	6.4-X
Solution I	10
Solution II 1 ul	1
Solution III	2
RNase inhibitor	0.6
Template DNA	700 ng (X)

2.23 Microfluidic chips

In order to make the microfluidic chip, first, we need to design the pattern on the silicon wafer, and rolling over and demold, there is a recessed microfluidic space on the PDMS. The side of the PDMS with the microfluidic is combined with the glass by oxygen

doi:10.6342/NTU202203638

plasma bonding, after that the channel will be located in the middle of the glass and PDMS (Figure 7).

1. Design the pattern and engrave on the silicon wafer.
2. PDMS pouring and curing on the silicon wafer.
3. Demolding and cutting of PDMS chip
4. Inlet and outlet drilling.
5. Plasma treatment: activation of glass and PDMS chip for binding.

2.24 Droplet formation

Use the pump to mix our sample and oil evenly into the microfluidic channel, and adjust the flow rate make the sample can be evenly wrapped in the oil droplets. Droplets were drawn from the outlet and placed on a slide (coated with a layer of PDMS) for observation with a fluorescence microscope (Figure 7).

doi:10.6342/NTU202203638

3. Result and discussion

The result can be divided into three aspects, one is the expression in E. *coli*, another is the proteins analysis, and the other is the expression in droplets. We used these three different aspects to explore the interactions and phenomenon between the Par complex proteins.

3.1 The expression in E. *coli*

The research data in this aspect can be divided into two parts, one is the synthesized proteins referred to the article (Liu et al., 2020) and the other is the proteins in different species form Fumio Motegi, can divided to these two parts.

For the part of synthesized proteins, first, we fuse the promoter (pTac or pLux) and fluorescent protein (sfGFP or mRFP) to the two synthesized proteins (Par-3N and Par-6β) through cloning. The final product of constructs design is showed in Appendix I.

For the expression of Par-3N in E. *coli*, we drive the protein with Tac promoter and fuse sfGFP fluorescent protein to help us observe the pattern with microscope, pTac-histag-sfGFP-Par3N. (Figure 8) We sub-cultured the construct at 37℃ and induced with different concentration of IPTG incubated in different time for fluorescence microscopy. In the end, we chose the concentration of 0.5 mM IPTG for subsequent experiments because there was a better phenomenon under this condition. We can observe that there

doi:10.6342/NTU202203638

were many multiple-foci formations in the E. *coli* (Figure 8B). The pattern is different from popZ which expression in E. *coli* was always unipolar. To promote the uni-polar foci formation, we tried to incubate the construct with the same concentration of IPTG for different induction time at 37℃. We can observe the value of polarity metric is gradually increase with induction times (Figure 8C). Although we can observe a positive correlation trend in this experimental result, but even at the longest induction time, the overall trend is still to form multiple-foci rather than unipolar-foci. According to the data we can predict that the aggregation ability of Par-3N may be poorer than that of popZ.

For the expression of Par-6β in E. *coli*, at the beginning we drive this protein with Bad promoter (Figure 9A). The pattern is diffusion in E. *coli* under the induction of 2% arabinose for 3 hours at 37°C, such pattern is in line with our expectations. In addition, we also cloned Par-6β (driven by Bad promoter) and Par-3N together (Figure 9B), but the result was that Par-3N still maintains multiple foci and Par-6β was still in a diffused state. There didn't seem to be any interaction between the two proteins. This result was not what we expected. But all in all, in the end, we found some problems in Bad promoter. So, we changed the promoter to Lux promoter. We sub-cultured the construct at 37℃ and induced with 0.01mM AHL (N-(3-Oxodecanoyl)-L-homoserine lactone)

doi:10.6342/NTU202203638

incubated for 3 hours. By the Lux promoter driven, we can observe there were unipolar-foci formation in E. *coli* (Figure 10). But this phenomenon is different from what we had expected. We had expected par-6β to be an assisting role, and par-3N to have the ability to self-aggregate, so we predict par-6β should be in a diffuse state and par-3N would observe foci formation, and the ability of par-3N to form foci in the presence of par-6β would be promoted. But the results of the current experiment were not the same as expected, par-6β would form a perfect unipolar foci in the presence of its own. Therefore, we cloned the two constructs of par-3N and par-6β together.

For the co-expression of Par-3N and Par-6β in E. *coli* (Figure 11), we observed that Par-6β still maintains a unipolar state, but Par-3N is very different. The ability of Par-3N to form foci has indeed been improved. Originally, in the case of expressing Par-3N alone, almost all we observed were the formation of multiple foci. However, after being expressed together with par6, all of them gradually formed unipolar foci. It can be seen that the ability of Par-3N to oligomerization has been significantly improved, and the Pearson correlation between the sfGFP-Par3N and mRFP-Par6β is as high as 0.93 (Figure 11C), which also proves that there is indeed an interaction between the Par-3N and Par-6β and the formation of unipolar is effectively improved under such interaction.

doi:10.6342/NTU202203638

In addition to the above analysis, we also detected the changes of this construct through the visually. As mentioned in the previous experimental results, in the case of expressing Par-3N alone, most of the experimental results were at the state of forming multiple foci. Therefore, we calculated the number and the types of foci by visually after induced both of the two constructs (Figure 12). According to the analyzed data, we could know that in the presence of Par-6β, the state of Par-3N to form unipolar foci increased significantly, so we could assert with certainty that Par-6β can effectively improve the oligomerization ability of Par-3N.

In addition, we also observed the difference between this construct before and after induction (Figure 13), because of the leakage of Tac promoter, in the state before induction we could find there were a little number of Par-3N foci were produced and because the Par-6β were not be induced, the foci of Par-3N was multiple foci (Figure 13B). However, after induce with IPTG and AHL, the prefect unipolar foci were formed (Figure 13B). This experimental result once again confirms our inference for Par-3N and Par-6β.

In addition to Par-3N and Par-6β, we also co-expressed Par-3 and Par-6 of C. *elegans.* (Figure 14) The construct was pLux-histag-mRFP-Par3_pTac-FLAG -sfGFP-Par6(r). From the results of the fluorescent signal, we could observe that some unipolar foci were formed (Figure 14B), but the two proteins of C. *elegans* still showed a certain

doi:10.6342/NTU202203638

ability of interaction, but most of the cases are still diffused (Figure 14D) and unipolar-foci occasional. (Figure 14C)

Comparing the above two sets of co-expressed experimental data, we found that Par-3N was truncated to retain only ntd and three pdz domains. Compared with Par-3N, we used the full length Par3 of the C. *elegans* group for the experiment.

Therefore, we speculate that if the less important domains in C. *elegans* Par3 are truncated and only important domains that interact with par6 are retained, the ability of the two proteins to interact will increase, and the ability to form foci will also increase. Therefore, we searched for the conservative domain of Par3 through the NCBI website (https://www.ncbi.nlm.nih.gov/Structure/cdd/wrpsb.cgi), and according to the results (Appendix IV), we truncated the unimportant area (755-1380 amino acid) behind it by cloning.

According to the fluorescence microscopy images (Figure 15), after truncation of the relatively unimportant domains of par3 in nematodes, the interaction with Par6 is improved, and the ability to form foci is improved. the Pearson correlation between the mRFP-Par3N and sfGFP-Par6β is as high as 0.77 (Figure 15C).

For the part of the Par proteins in different species form Fumio Motegi, the fragments

doi:10.6342/NTU202203638

would be sequenced immediately to confirmation the sequence and then also would be fused the promoter (pTac or pLux) and fluorescent protein (sfGFP or mRFP) through cloning. The final product of constructs design is showed in Appendix II-IV.

First of all, we looked the expression of Par-3 (C. *elegans*) in E. *coli* (Figure 16), we could find that a small amount of unipolar foci were formed, but most of the expression still in the state of diffusion (Figure16B). After fluorescence intensity analysis (Figure 16C), the overall data was also in the state of diffusion, but through the quantification of fluorescence intensity we can know that protein is indeed induced.

Next, we looked the expression of Par-3 (sea anemone) in E. *coli* (Figure 17), we could observed the proteins diffuse in the strains (Figure 17B). After fluorescence intensity analysis (Figure 17C), the data was also diffusion. And after the induction, the fluorescence intensity was increased, so the construct was indeed produced.

Third, we looked the expression of Par-3b (human) in E. *coli* (Figure 18), In the performance of this construct, we could also observe that all were in a state of diffusion (Figure 18B). After fluorescence intensity analysis (Figure18C), the data also presented diffusion. And we know the construct indeed be induced by the fluorescence intensity matrix.

Then, we looked the expression of Pard-3 (mouse) in E. *coli* (Figure 19), In the

doi:10.6342/NTU202203638

performance of this construct, we could find a small quantity of unipolar foci were formed, but most of the expression still in the state of diffusion (Figure 19B). After fluorescence intensity analysis (Figure 19C), the data also presented diffusion. And we make sure the construct indeed be induced by the quantification of fluorescence intensity data.

Last, the 100kDa isoform of Pard-3 (mouse) was also expressed in E. *coli* (Figure 20), In the performance of this construct, still in the state of diffusion (Figure 20B). After fluorescence intensity analysis (Figure 20C), the data also presented diffusion. And we make sure the construct indeed be induced by the quantification of fluorescence intensity data.

Next, we focused on Par-6, Par-6 (C. *elegans*) expressed alone in E. *coli*, driven by Lux promoter and induced by AHL, could form a very beautiful unipolar foci like Par-6β (Figure 21). But the data is different from the Par-6 (C. *elegans* cDNA in yeast codon optimization). The data was almost diffusion state in yeast codon optimization construct (Figure 22).

Since we also wanted to study co-expression of Par-3 and Par-6 (C. *elegans*), pLux-histag-mRFP-Par3_pTac-FLAG -sfGFP-Par6(r) (Figure 14). We first replaced Par-6 construct's the promoter with Tac promoter and fuse FLAG tag and sfGFP fluorescent proteins. The fluorescent image data was showed on Figure 23. And the yeast codon

doi:10.6342/NTU202203638

optimization fluorescent image data was showed on Figure 24. We could find that the construct driven by Tac promoter were different from driven by Lux promoter. The data driven by Tac promoter were almost diffusion. The analysis of the Par-6 seem to not induce successfully. The P value is 0.24 means that there is no significantly different between before and after induction. But the sequencing result was correct so it may need to more study about this construct. But anyway, we still temporarily used this construct to synthesize pLux-histag-mRFP-Par3_pTac-FLAG -sfGFP-Par6(r) (Figure 14).

In this part of the data, although most of the constructs of Par-3 showed diffusion, a few unipolar foci were still observed, and the related experiments need to further testing.

doi:10.6342/NTU202203638

3.2 Protein gel analysis

In addition to the above-mentioned performance systems, we also further assist us in the study of Par proteins through protein experimental techniques. The experiments in this part could also be divided into two aspects. The first aspect is that our previous experiments in E. *coli* expressing Par-3N (rat) /Par-6β (mouse) and Par-3/ Par-6 (C. *elegans*) showed that there was colocalization between Par-3 and Par-6, but we observed that the group of par3/par6 in C. *elegans* experiments was not too stable, so we want to directly explore the interaction between the two proteins through the analysis of protein technology e.g. Co-Immunoprecipitation (Co-IP) and Western blotting experiments ; Another part of the experiment is to study Par-3. Due to the structure of Par-3, many literatures clearly pointed out that Par-3 has the ability of oligomerization (Feng et al., 2007; Liu et al., 2020; Thompson, 2022; Wu et al., 2007), thus we also wanted to study the ability to self-oligomerize of Par-3 through protein experimental technology. Here we also used various Par-3 homologues in different species form Fumio Motegi to carry out this part of the experiment. And we expect to explore the ability of Par-3 to self-aggregate by comparing the experimental results of SDSPAGE and NATIVE PAGE.

First, for the two aspects of protein experiments, we fuse the protein tags (6x his-tag or FLAG tag) to the constructs through cloning. The final product of constructs design is

doi:10.6342/NTU202203638

showed in Appendix I-III.

First, we have to test if the Immunoprecipitation works effectively, we used the PopZ, pLux-histag-mRFP-PopZ and PopZ (delta 134-177)(Holmes et al., 2016), pLux-histag-mRFP-PopZ (delta 134-177) to check this system. From the SDS PAGE (Figure 25), we could find that the bands after elution were equal to the major band of cell lysates in these two samples. So, we could know that the Immunoprecipitation system can work. Then we need to study the ability to oligomerize of Par-3, we used various Par-3 homologues in different species form Fumio Motegi to carry out this part of the experiment. At first, we run the SDS PAGE electrophoresis to separate the lysate. We used the construct pLux-histag-mRFP-PopZ as our positive control. Then we ran the Par-3 of the two species (C. *elegans* and anemone) at first and analyzed by Western blotting with anti-His tag antibody (Figure 26 B).

Then switch to Par-6 data (Figure 27), the three construct, Par-6β, Par-6 of C. *elegans* and C. *elegans* cDNA in yeast codon optimization (Figure 27A). The kDa of the last two should be the same (Figure 27B lane 2 and 3). Then we ran SDS PAGE these three constructs and analyzed by Western blotting with anti-FLAG tag antibody (Figure 27B). From the results of Western blotting, we could know that most of the bands appeared in membrane larger than the molecular weight we predicted. We infer that because our samples have the ability to oligomerization, so just relying on SDS may not be enough

doi:10.6342/NTU202203638

to inhibit the polymerizing ability of the protein itself. Therefore, if we need to conduct more accurate experiments, it may be necessary to pre-process the samples, such as urea or iodoacetamide. There are still samples of some species that have not been tested, so follow-up experiments need to continue.

Besides the SDS PAGE, our ultimate goal is to run the native page, because the native page can see whether there will be various isoforms, and compare the results between the SDS PAGE and the NATIVE PAGE to study the oligomerization ability of different species Par-3. But after many tests, there are still some problems that need to be solved in the experiment of running NATIVE PAGE. Running a single concentration of gel is not enough to do this, so we need to test the method how the native page gradient gel be made, so experiments in this aspect still require a lot of testing.

For another part of study, we used the construct “pLux-FLAG-mRFP-Par6β-pTac-histag-sfGFP-Par-3N(r)” to conduct Co-Immunoprecipitation (Co-IP) experiments (Figure 28). The experiments could be divided into three groups. The first group was induced by AHL only to drive” FLAG-mRFP-Par6β”; the second group was induced by IPTG only to drive” histag-sfGFP-Par-3N”; and the third group was induced by both inductions to drive” histag-sfGFP-Par-3N” and” FLAG-mRFP-Par6β” at the same time. These three groups were under the same experimental environment and conditions,

doi:10.6342/NTU202203638

subculture, induction and harvesting centrifugation were carried out at the same time. From the experimental results, we could first observe that when two inducers are added at the same time (Figure 28C lane 3) (group 3), we could see that there was a clear band approximately 75kDa in size which was close to the predicted molecular weight of Par-6β (68kDa). This result could demonstrate that Par-3N linked 6x-Histag indeed has a strong interaction with Par-6β linked FLAG-tag, so that after purification pulldown by His tag, anti-FLAG antibody could probe the band of Par-6β.

Next, we turned our attention back to the second group that only added IPTG for induction (Figure 28C lane 2). The results of the experiment were very in line with our expectations. It could be found that the results were very clean and no bands appeared. Because we used anti- FLAG antibody to probe, but no induce FLAG-mRFP-Par6β just expressed histag-sfGFP-Par-3N alone. Therefore, after purification and pulldown by His tag, the anti- FLAG antibody cannot detect anything.

Finally, we saw the first group that was only induced with AHL (Figure 28C lane 1). Logically, because only the expression of FLAG-mRFP-Par6β was induced, in the absence of His tag, no protein should be obtained after purification and pulldown, so there should no band could be detected by the anti- FLAG antibody. But unexpected, we observed a faint band near 75kDa in size which was close to the predicted molecular weight of Par-6β (68kDa). Here we infer that the Tac promoter has a strong leakage, so

doi:10.6342/NTU202203638

even in the absence of IPTG induction, it would expressed Histag-sfGFP-Par-3N slightly, resulting in a small amount of proteins obtained after purification and pulldown, and the experimental results were also very in line with our expectations.

Summarizing the results of the above three groups of experiments, we demonstrated the relationship through protein analysis experiments. We once again proved that there was indeed an interaction between the two proteins Par-3N and Par-6β.

Another group to study the interaction was par3/par6 in C. *elegans* experiments, but in this group, we have some issues need to trouble shooting.

doi:10.6342/NTU202203638

3.3 The expression in droplet system

In addition to the above two systems, we also try to perform in cell-free systems such as droplet system. At present, we have tested two experimental methods. The first is to use IVTT kit to make our target proteins to be translated and transcribed *in vitro*, and then wrap it in the droplets to observe the performance; and another experimental way is to directly wrap the cell lysate into the oil droplets.

Before using IVTT, we had to transform the two T7 promoter constructs into the BLR (DE3) to check the performance *in vivo* (Figure 29). The image showed that both the sfGFP-Par-3N and mRFP-Par6β were diffuse in this strain.

The results of IVTT experimental system were be showed in Figure 30. We can observe there were foci formation in the droplets. First, Popz is recognized as a protein with strong self-polymerization ability, so we used this protein as our positive control group in this experiment. The protein was driven by T7 promoter and fused sfGFP help us find the phenomena, pT7-sfGFP-popZ. After packaged this construct into the droplets by IVTT, we can observe obvious foci formation through green fluorescence, and most of the foci were aggregated near the edge of each oil droplet (Figure 30A). Then we focus back on the Par-3N protein, we can find that after being driven by the T7 promoter, we could also find the formation of foci in the droplets (Figure 30B). Compared to

doi:10.6342/NTU202203638

PopZ, the amount of foci produced was much less and most of the foci were not formed near the edge of droplets. Such experimental results once again confirm our speculation: the aggregation ability of Par-3N is indeed much inferior to that of PopZ, and it may need the assistance of Par-6β to have a higher oligomerization ability.

Therefore, we next turned our attention to the performance of Par-6β (Figure 30C). In the beginning, we used mRFP as a fluorescent protein, but after several tests, we still could not observe the performance of fluorescent signals in droplets through IVTT, so we finally changed mRFP to mCherry for subsequent experiments. In previous experiments expressing Par-6β in E. *coli*, we observed very beautiful unipolar foci formation, and compared to the E. *coli* data, we could also find that in droplets. The formation of foci was observed and some of the foci formed a crescent-shaped at the edge of the droplets, but also compared with the experimental results of PopZ, the yields of foci formed was still relatively less.

Finally, we also expressed the two proteins sfGFP-Par-3N and mCherry-Par6β together in the droplets (Figure 30D). We wanted to verify whether the polymerization ability of Par-3N would be significantly improved in the presence of Par-6β. But unfortunately, in the experimental results of mixing two proteins sfGFP-Par-3N and mCherry-Par6β, the performance of mCherry-Par6β, the fluorescent signals were always been weak, while sfGFP-Par-3N was normal, so we had not observed more successful experimental

doi:10.6342/NTU202203638

results. Our preliminary inference is that: Since the final total volume of IVTT must be maintained, the same volume must be allocated to the solution of the two proteins, so the DNA concentration contained in it may be less than in the case of individual performance, resulting the final production of protein production was reduced made we cannot observe the performance of the proteins. There are two solutions for troubleshooting. The first is to directly cloned the two constructs together, by that these two proteins can be expressed at the same volume at the same time, but because the promoter carried by them are the same, the cloning method will be more difficult; the second is to concentrate the DNA, so that at the same volume can have a higher amount of DNA can solve the problem of insufficient DNA concentration. Both methods require more follow-up tests and discussions.

Another prepare samples method was the cell lysate experimental system (Figure 31). In this system, we first expressed the two constructs pTac-histag-sfGFP-Par-3N and pLux-FLAG-mRFP-Par6β in E. *coli*, after subculture and induced with 0.5mM IPTG and 0.01mM AHL incubated at 37℃ for 6 hours, lysis the cell, and directly wrapped the cell lysate into the droplets to observe the performance. We could observe the fluorescent signals in the droplets so we could be sure that both proteins were indeed expressed. We also find some foci in the droplets of sfGFP-Par-3N (Figure 31A).

doi:10.6342/NTU202203638

Compared to sfGFP-Par-3N, the fluorescent signals in mRFP-Par6β were presented in the form of diffusion (Figure 31B). The results were different from IVTT system. In addition to the two constructs, we also sent the cell lysate of combined product by cloning, pLux-FLAG-mRFP-Par6β_pTac-histag-sfGFP-Par-3N(r) to the droplets for expression (Figure 31C). We originally expected that the experimental results would be the same as the experiments performed in E. *coli*, we may see that the two proteins have a very high-level interaction and produce phenomenon of LLPS in the droplets system. But the results were not what we expected. Although both proteins were indeed expressed, it seemed that no interaction was observed between the two proteins. The fluorescent signals of two constructs were almost in the state of diffusion, and the ability of Par-3N oligomerization seem didn't to be improved. We require more tests and discussions about the results.

We also observed some phenomena in the droplet system experiments, first, compared with IVTT solution, cell lysate can form smaller droplets. The reason may be related to the viscosity of the solution.

Another question in the IVTT system, the droplets are formed first and then make the proteins incubate in droplets for 3hrs, or first incubated the proteins outside for 3hrs then warped into droplets, is there any difference in the distribution of fluorescence?

doi:10.6342/NTU202203638

For this result we give the following preliminary explanation: because of the final volume is the same, the ability to form foci for monomers or dimers may not be bad, but for oligomers, there may be differences due to the collision probability.

Last question, after the pLux-Flag-mRFP-par6β cell lysate was packaged into the droplet, we observed a fluorescent signal; but no fluorescence was generated when the T7-mRFP-par6β construct was added. It is preliminarily speculated that in the cell-free system, the presence or absence of fluorescent signals is related to the efficiency of protein folding because the folded mRFP emitted light when it is package into the droplet, but it was not observed in the IVTT system.

doi:10.6342/NTU202203638

4. Conclusion and future work

According the series of experimental results, we successfully expressed the PAR protein complex in E. coli and droplets, and successfully observed the foci formation. And we also observed in the presence of Par-6β, the state of Par-3N to form unipolar foci increases significantly, so we demonstrate certainty that there exists strong interaction between Par-6β and Par-3N and Par-6 can effectively improve the oligomerization ability of Par-3N.

According to our data, we can observe a phenomenon that the foci of PopZ is always unipolar but when expressing Par-3N along the foci always multiple-foci. Both of the PopZ and Par-3 have the ability to self-oligomerization. By the data, we can know that the aggregation ability of Par-3 may be poorer than that of PopZ, and this may be the tendency in higher organisms to use the second protein to help promote the oligomerization of the main protein.

In this study, we used three different systems" E. *coli* system, droplet system and pure protein analyses to discuss the PAR complex, and the research results of the three systems have some points that can confirm each other and some points that are different from each other. However, the three systems also had their own problems that must be solved. For example, (1) in the E. coli experiment, the experimental results driven by different promoters were inconsistent with each other; and (2) in the droplet system, the

doi:10.6342/NTU202203638

unstable fluorescent signal must be solved. (3) Finally, in the protein gel system, the problem of NATIVE gradient gel must be solved in order to be compared with the SDS PAGE, so that we could explore the self-oligomerization ability of Par proteins of different species.

Therefore, the direction of the next step of this project may be towards the integration of these three different systems. We must first solve the respective problems of the three systems and then compare and integrate the results of the three systems. Ultimately, it is possible to further and clearly describe the workings of the par complex as a whole.

doi:10.6342/NTU202203638

5. Figure

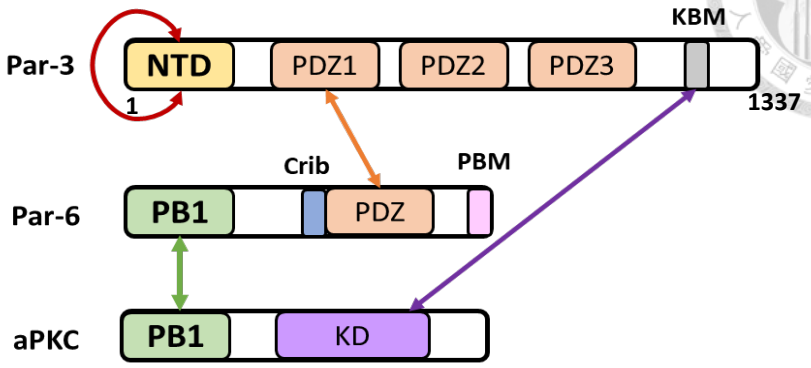

Figure 1. Schematic diagrams the domain organizations and interactions (arrows) within the par complex. PDZ-binding motif (PBM); atypical protein kinase C (aPKC); N-terminal domain (NTD); kinase binding motif (KBM); kinase domain (KD)

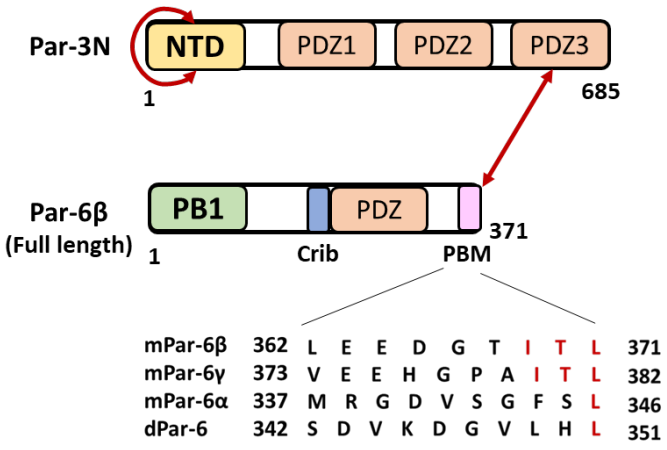

Figure 2. Schematic diagrams showing the domain organizations of Par-3N and Par-6β. Par-3N is a truncated form of Par-3 (rat) containing NTD and PDZ domains 1-3. Amino acid sequences of the PBM in mouse α, β, γ and *Drosophila* Par-6 are showed.

doi:10.6342/NTU202203638

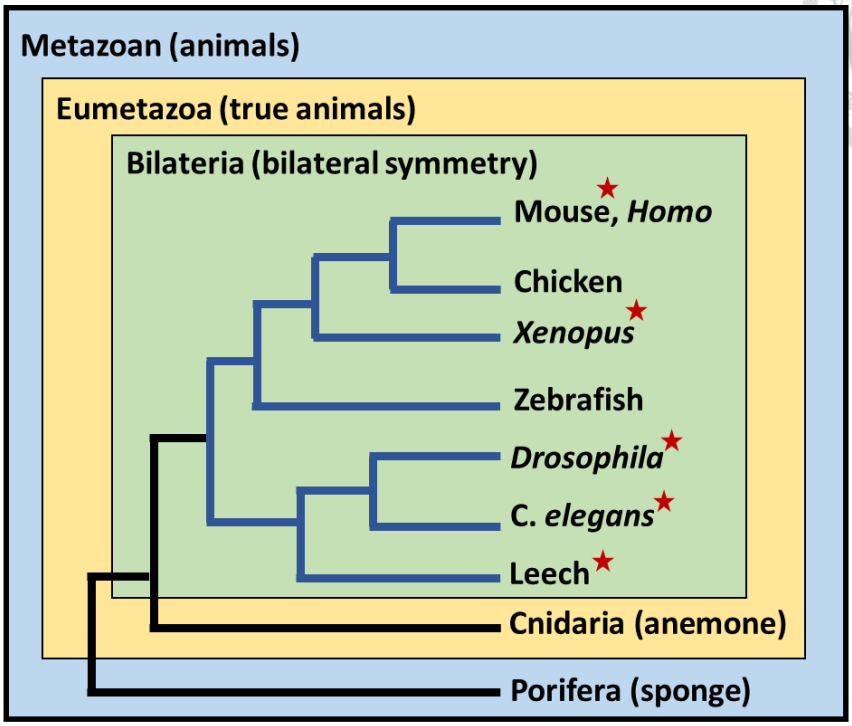

Figure 3. PAR protein complex is conserved in the genome of sequenced Metazoan. The function of PAR proteins has only been described in some bilateral animals, and no relevant description can be found in the literature in non-bilateral animals. The blue branches indicate that the function of PAR proteins in epithelial has been described. The red stars represent that the function of PAR proteins in early embryogenesis has been described.

doi:10.6342/NTU202203638

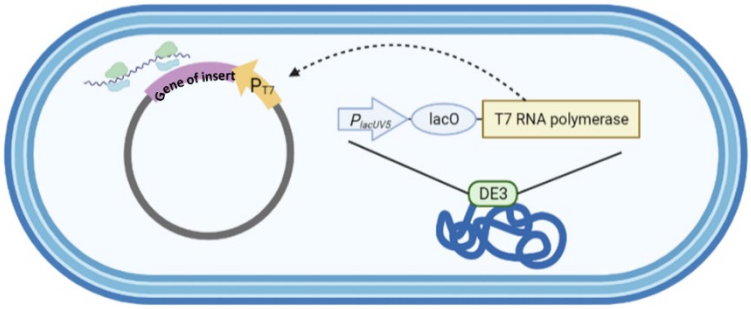

Figure 4. The schematic diagrams showing the work of BLR (DE3) competent cell after induction with IPTG

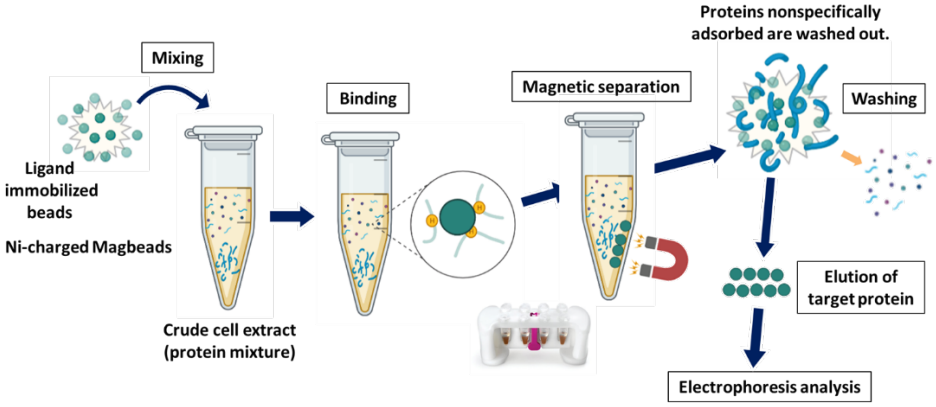

Figure 5. The schematic diagrams showing the principle of Immunoprecipitation (IP).

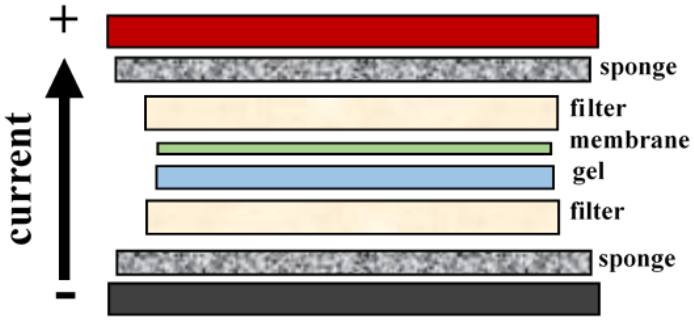

Figure 6. The schematic diagrams showing the preparation of Western bolt transfer stack.

doi:10.6342/NTU202203638

(A)

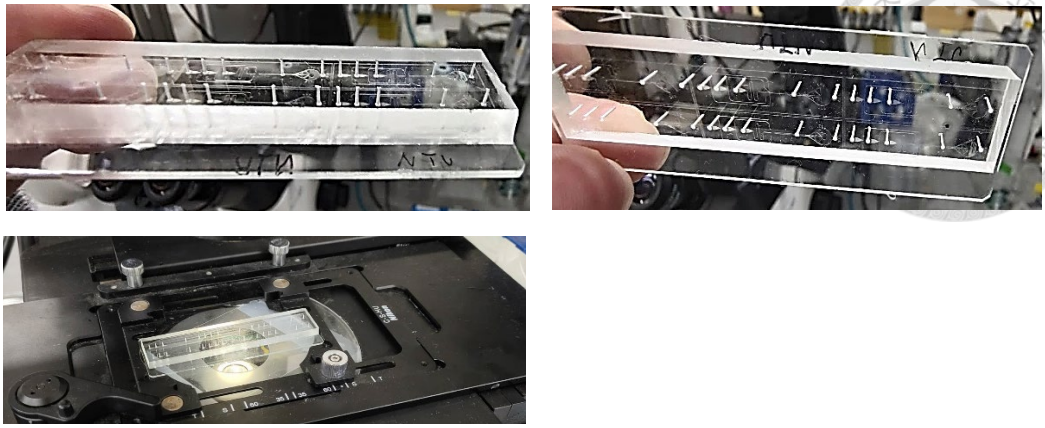

(B)

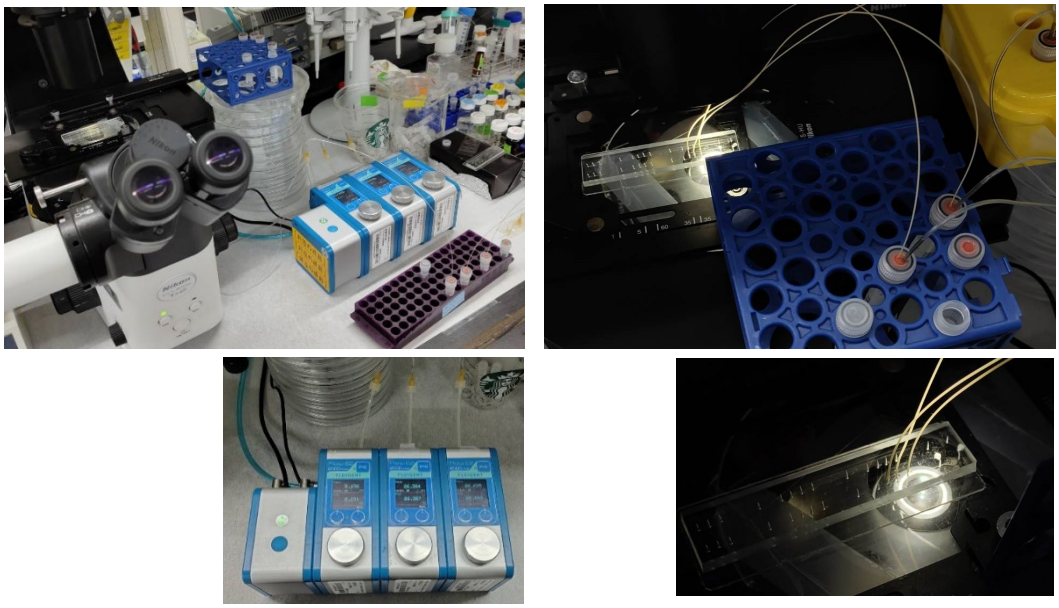

(C)

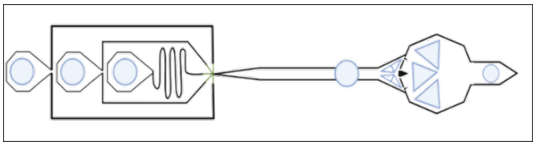

(D)

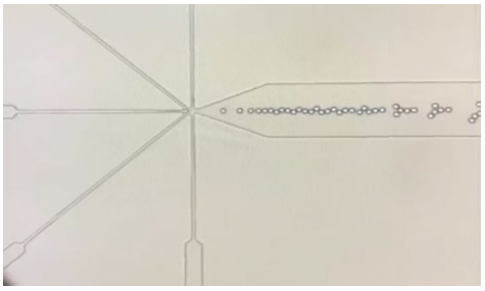

Figure 7. Image of prepared droplet system. (A) The finished PDMS product of the microfluidic chips. (B) Experimental equipment erection of droplet formation. (C) The schematic of real-time droplet ratio-tunable chip. (D) The bright field image of the formation of droplets under the microscopy.

doi:10.6342/NTU202203638

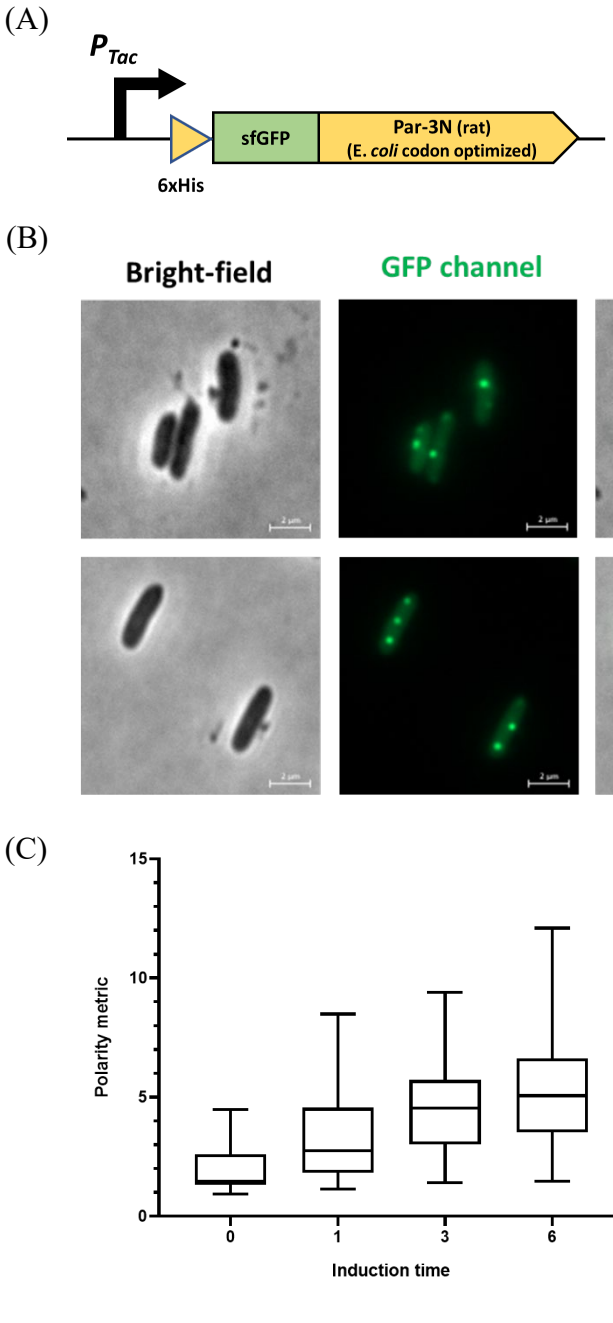

Figure 8. The fluorescence microscopy images for pTac-his-sfGFP-Par 3N. (A) The construct diagrams. (B) The fluorescence microscopy images of pTac-his-sfGFP-Par3N. The condition is induce by 0.5 mM IPTG and incubate at 37℃ for 3 hours. (C) The value of polarity metric with different induction times.

doi:10.6342/NTU202203638

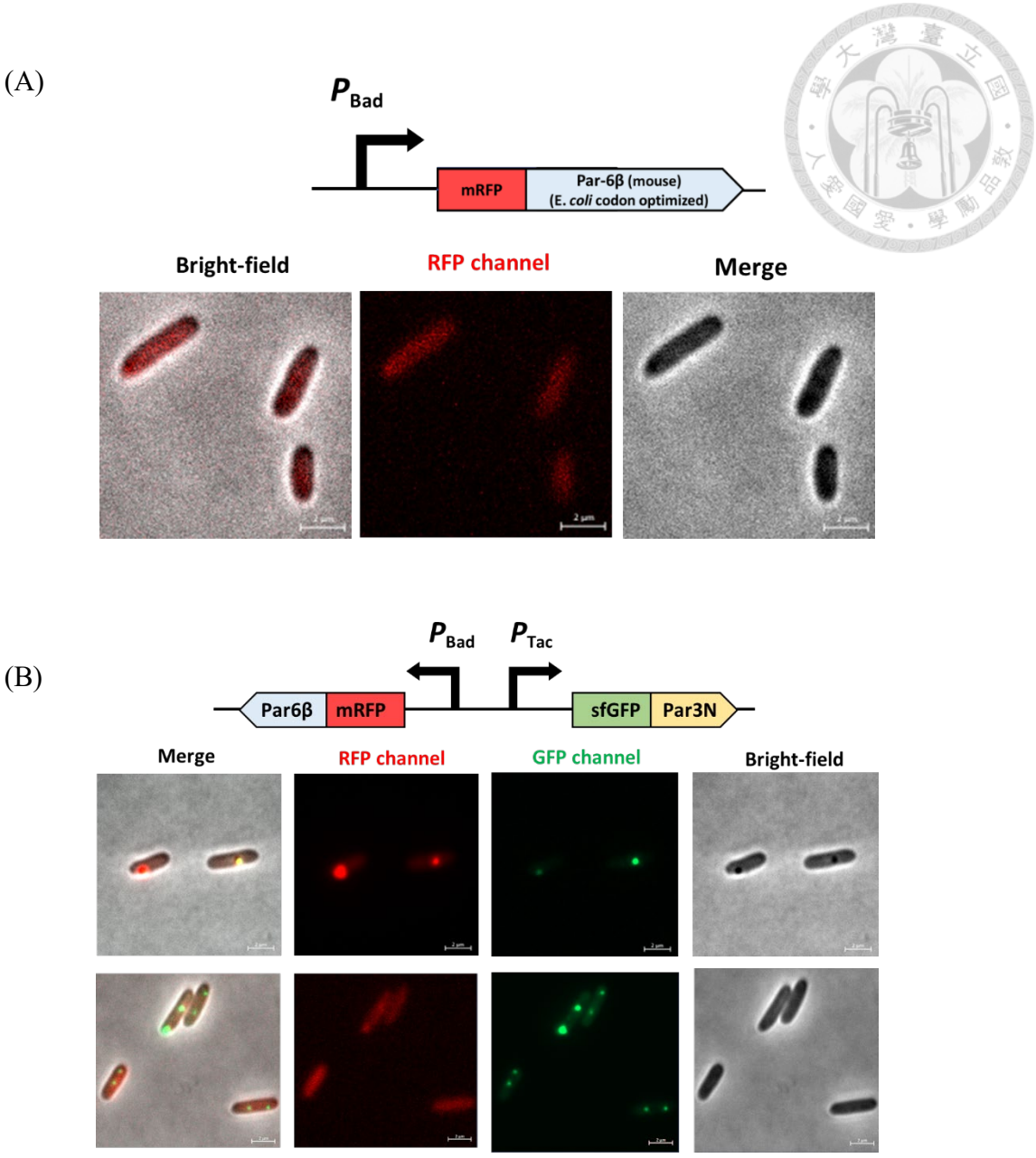

Figure 9. The expression of Par6β driven by BAD promoter system in *E. coli.* (A) The expression of Par6β alone, pBAD-mRFP-Par6β. (B) The co-expression of Par3N and Par6β, pTac-sfGFP-Par3N_pBAD-mRFP-Par6β(r). Induce by 2％ arabinose for 6 hours at 37˚C. the unipolar foci (top images) were occasional and diffusion (bottom images) were majority.

doi:10.6342/NTU202203638

(A)

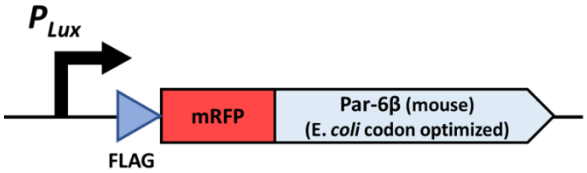

(B)

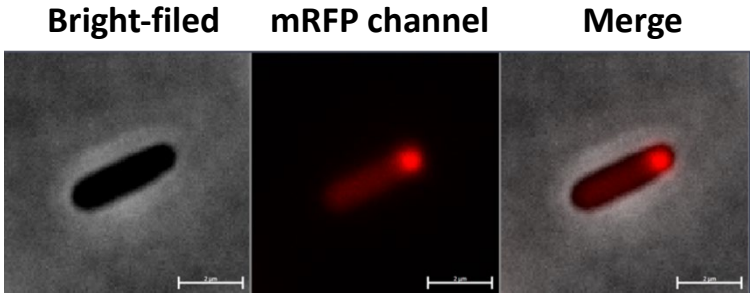

(C)

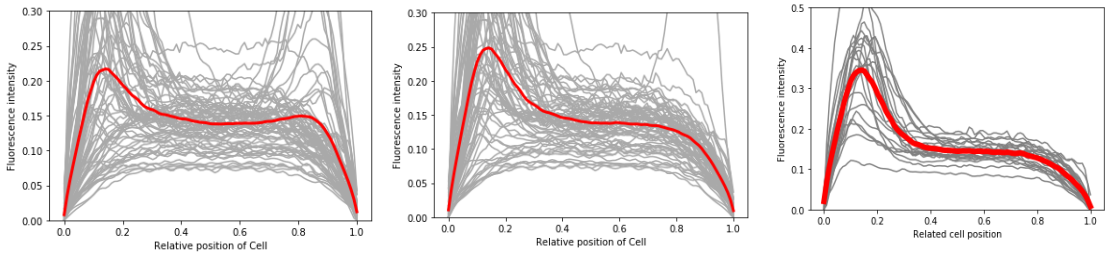

Figure 10. The expression of Par6β in *E. coli.* (A) The construct diagrams. (B) The fluorescence microscopy images of pLux-FLAG-mRFP- Par6β. Induce by 0.01mM AHL and incubate at 37℃ for 3 hours. (C) Fluorescence intensity (mRFP) profiles along the axis of cell. Fluorescence intensity (mRFP) profiles along the axis of cell. Induce for 3 hours (left image). The intensity was flipped to the same side (middle image). And the fluorescence intensity data analysis by Otsu's thresholding method (right image). The fluorescence intensity normalized by the maximal. Gray lines mean that fluorescence intensity of a cell. The red lines indicate averages.

doi:10.6342/NTU202203638

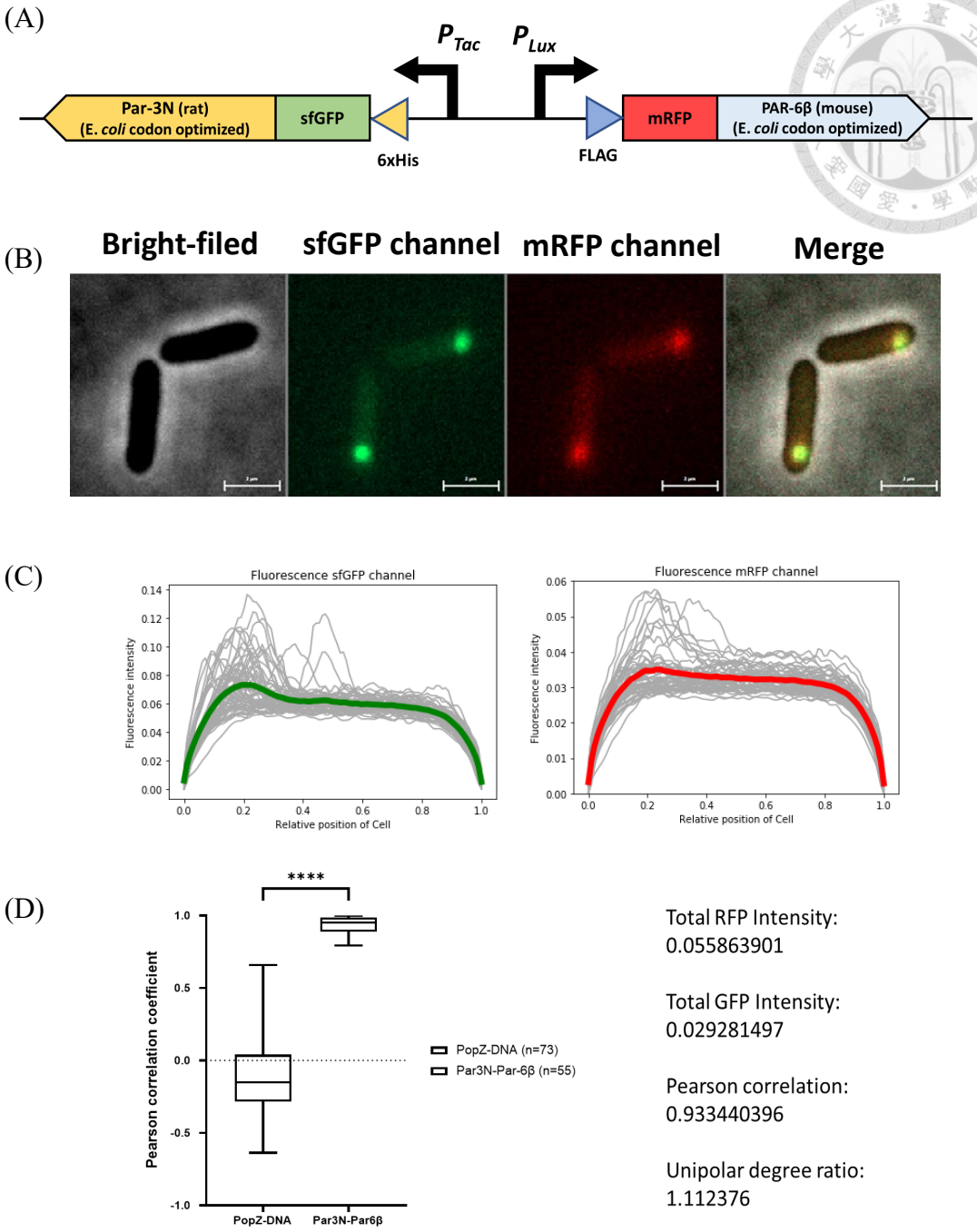

Figure 11. The expression of Par3N and Par6β combine in *E. coli.* (A) The construct diagrams. (B) The fluorescence microscopy images of pLux-FLAG-mRFP- Par6β-pTac-his-sfGFP-Par3N(r). Induce by 0.01mM AHL and 0.5mM IPTG, incubate at 37℃ for 3 hours. (C) Fluorescence intensity (sfGFP and mRFP) profiles along the axis of cell. The fluorescence intensity normalized by the maximal.

doi:10.6342/NTU202203638

Gray lines mean that fluorescence intensity of a cell. The green and red lines indicate averages. (D) Quantification of the Pearson correlation between the sfGFP-Par-3N and mRFP-Par6β. PopZ-DNA negative control. Statistical difference was determined by Student's t-test; **** means that the P value < 0.0001.

doi:10.6342/NTU202203638

	Par-3N only
Unipolar	**27.7% (n=23)**
Multiple-polar	**72.3% (n=60)**
Total	**100% (n=83)**

	Par-3N + Par-6β
Unipolar	**94.8% (n=73)**
Multiple-polar	**5.2% (n=4)**
Total	**100% (n=77)**

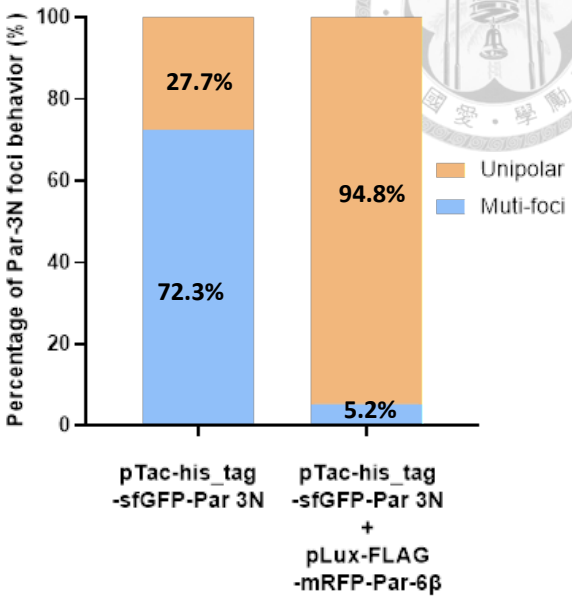

Figure 12. Detected the changes of foci state in this construct pLux-FLAG-mRFP-Par6β-pTac-his-sfGFP-Par3N(r) through the visually.

doi:10.6342/NTU202203638

(A)

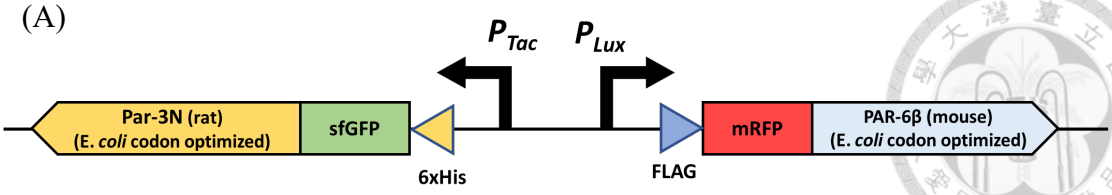

(B)

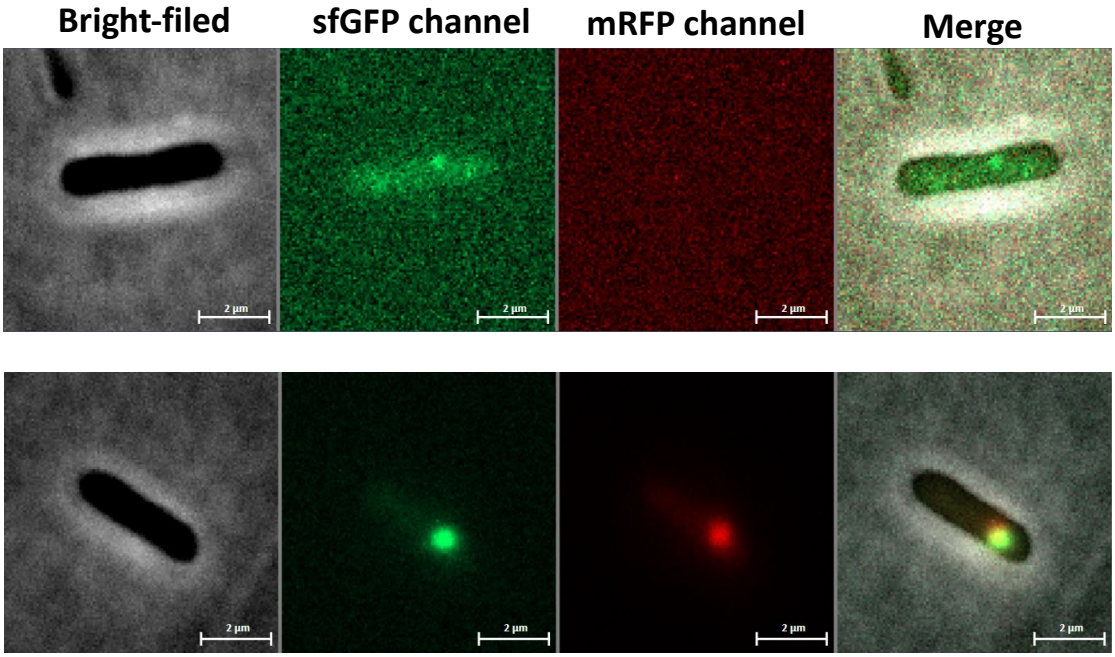

Figure 13. The expression of Par3N and Par6β combine in *E. coli.* (A) The construct diagrams. (B) The fluorescence microscopy images of pLux-FLAG-mRFP- Par6β-pTac-his-sfGFP-Par3N(r). Before induction, driven by leakage of pTac promoter (top image). Induce by 0.01mM AHL and 0.5mM IPTG, incubate at 37℃ for 3 hours. (bottom image)

doi:10.6342/NTU202203638

(A)

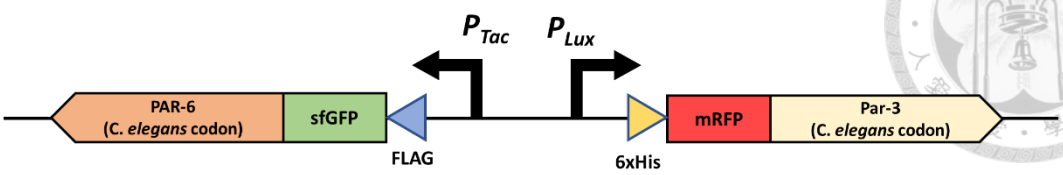

(B)

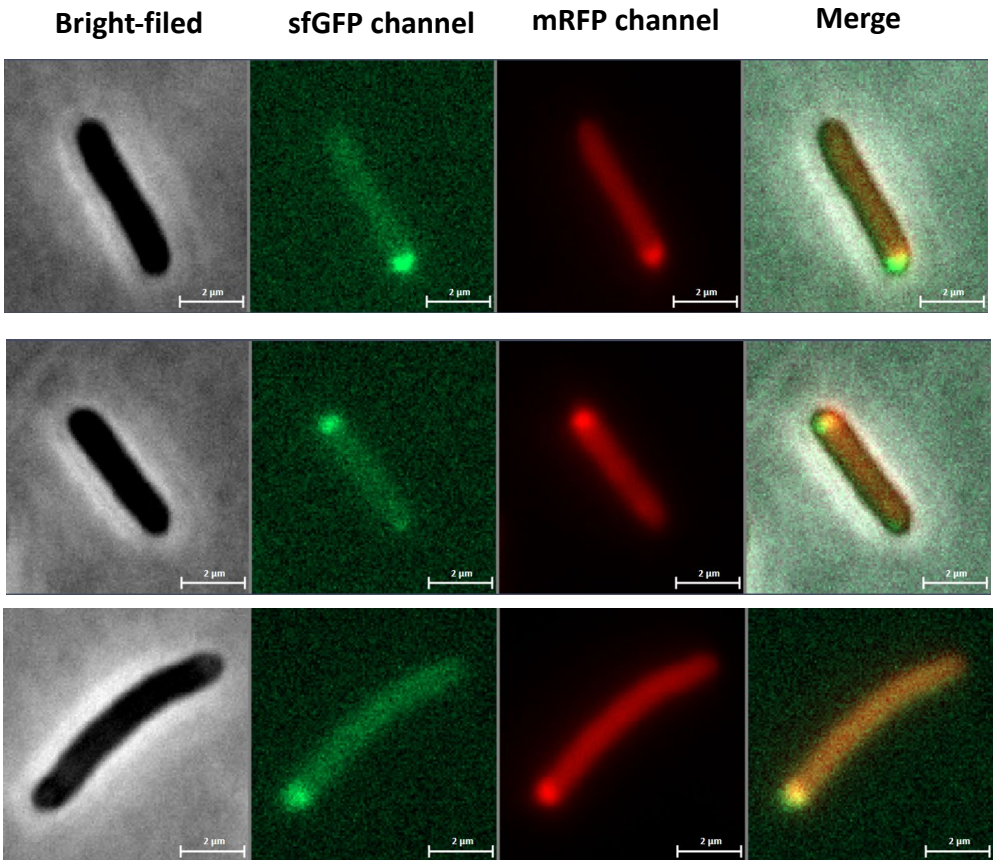

(C)

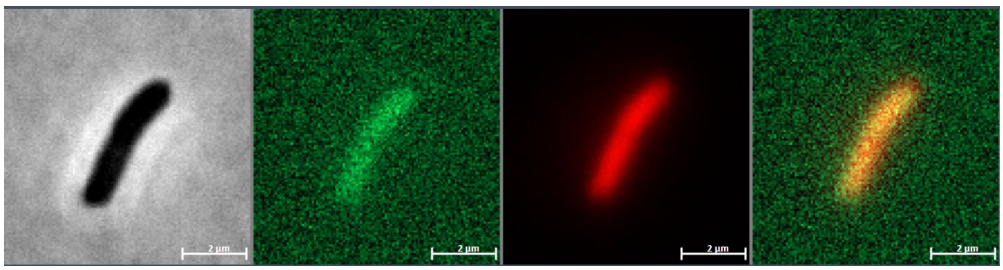

doi:10.6342/NTU202203638

Figure 14. The co-expression of C. *elegans* Par3 and Par6 combine in E. *coli.* (A) The construct diagrams. (B)(C) The fluorescence microscopy images of pLux-histag-mRFP-Par3_pTac-FLAG-sfGFP-Par6(r), the diffusion (B) is majority and unipolar foci (C) is occasional. Induced by 0.5mM IPTG and 0.01mM AHL incubated at 37℃ for 3 hours.

doi:10.6342/NTU202203638

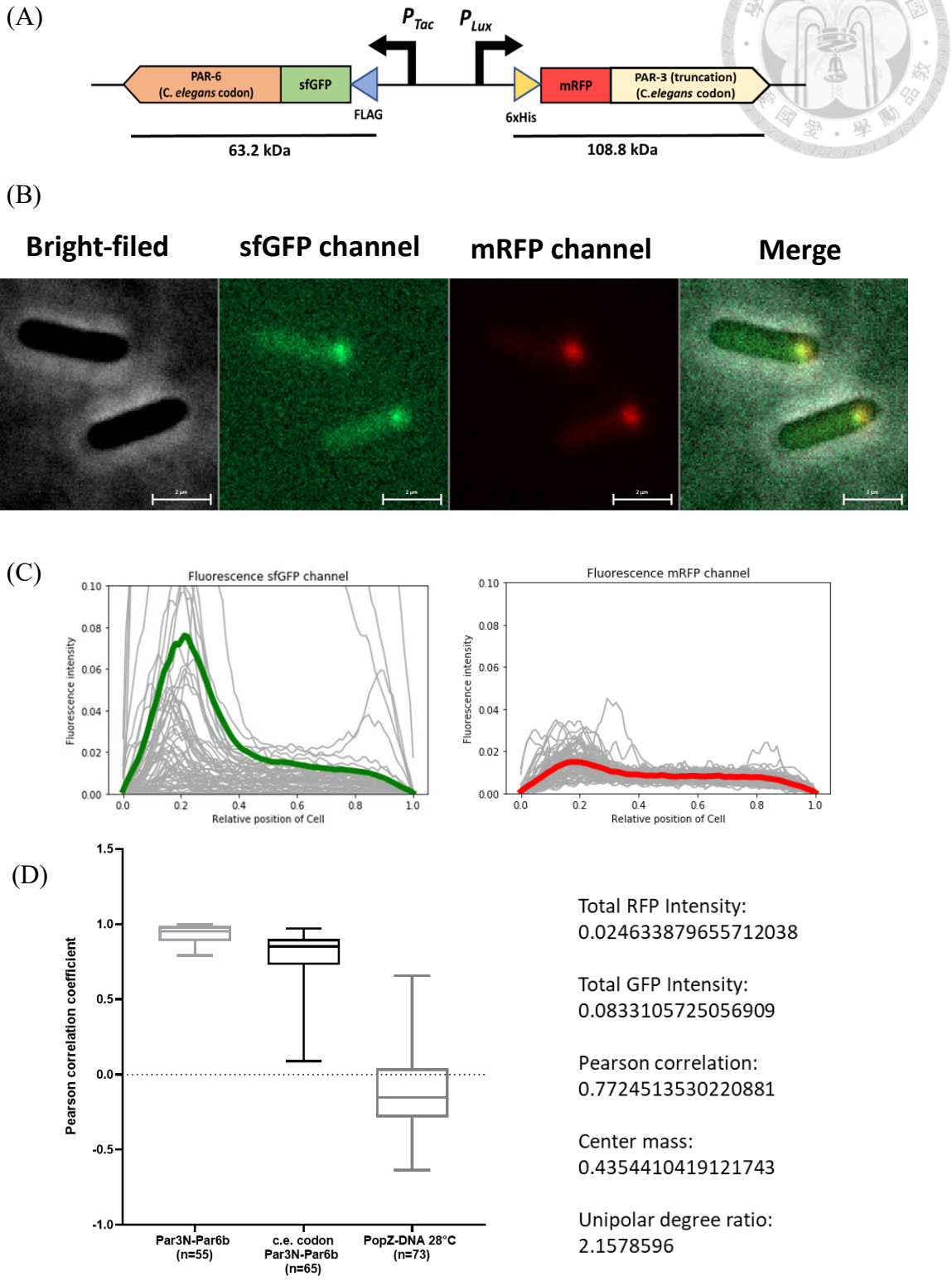

Figure 15. The co-expression of C. *elegans* Par3 (truncation) and Par6 combine in E. *coli.* (A) The construct diagrams.

doi:10.6342/NTU202203638

(B) The fluorescence microscopy images of pLux-his-mRFP-Par3(truncation)-pTac-his-sfGFP-Par6(r). Induce by 0.01mM AHL and 0.5mM IPTG, incubate at 37℃ for 3 hours. (C) Fluorescence intensity (sfGFP and mRFP) profiles along the axis of cell. The fluorescence intensity normalized by the maximal. Gray lines mean that fluorescence intensity of a cell. The green and red lines indicate averages. (D) Quantification of the Pearson correlation between the mRFP-Par3 and sfGFP-Par6. PopZ-DNA negative control. Statistical difference was determined by Student's t-test; **** means that the P value < 0.0001.

doi:10.6342/NTU202203638

(A)

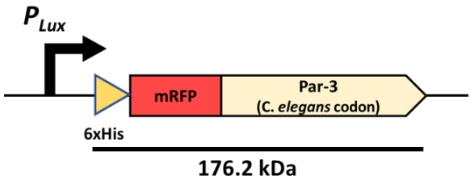

(B)

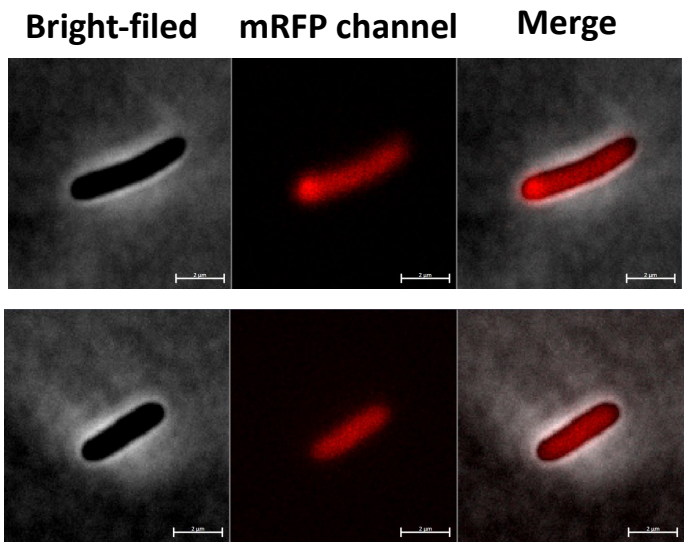

(C)

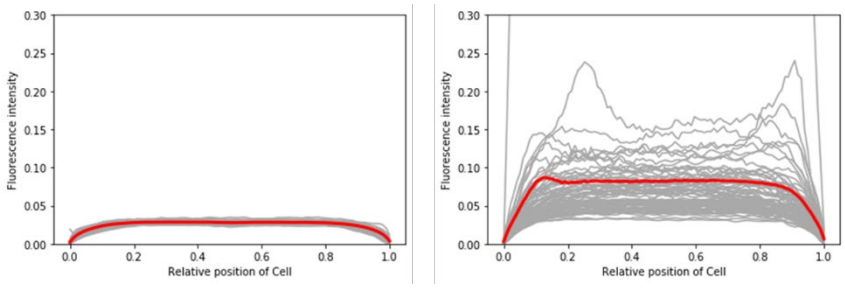

(D)

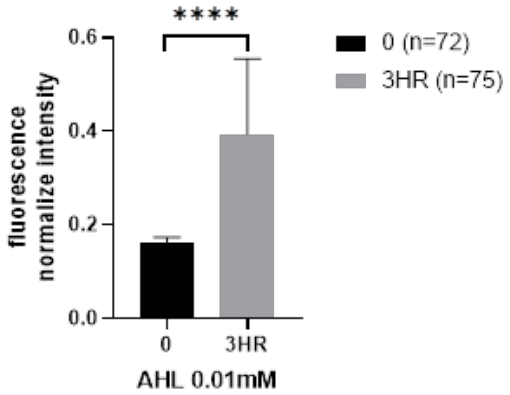

Figure 16. The expression of the C. *elegans* Par3 in E. *coli.* (A) The construct diagrams. (B) The fluorescence microscopy images of pLux-his-mRFP-Par3. Induce by 0.01mM AHL and incubate at 37℃ for 3 hours.

doi:10.6342/NTU202203638

(C) Fluorescence intensity (mRFP) profiles along the axis of cell. Before the induction (left image) and induce for 3 hours (right image). The fluorescence intensity normalized by the maximal. Gray lines mean that fluorescence intensity of a cell. The red lines indicate averages. (D) Quantification of the normalize fluorescence intensity The Statistical difference was determined by Student's t-test; **** means that the P value < 0.0001.

doi:10.6342/NTU202203638

(A)

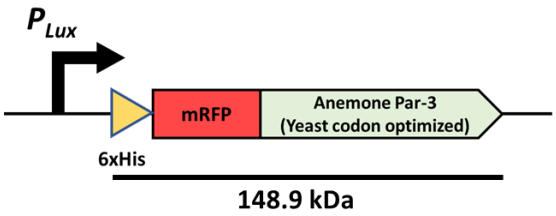

(B)

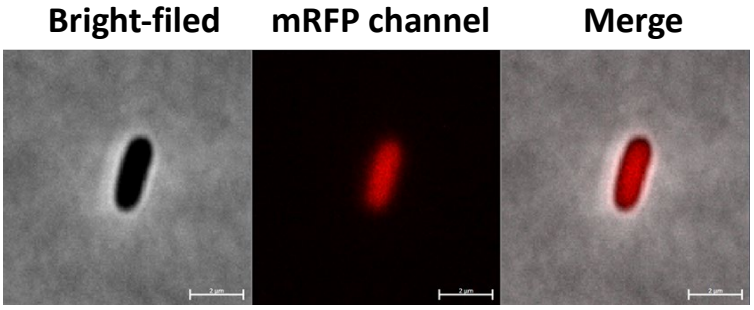

(C)

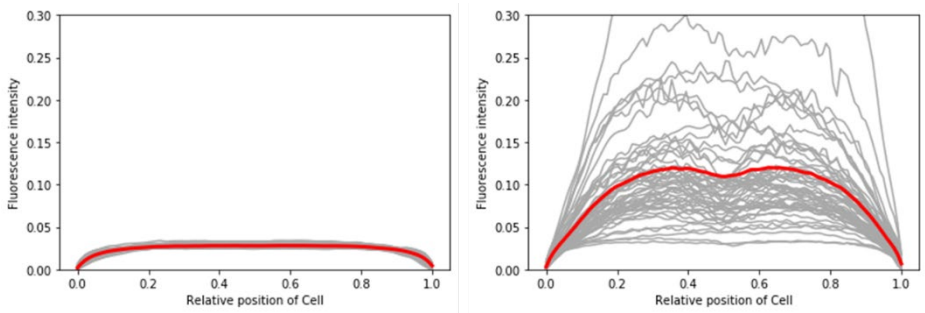

(D)

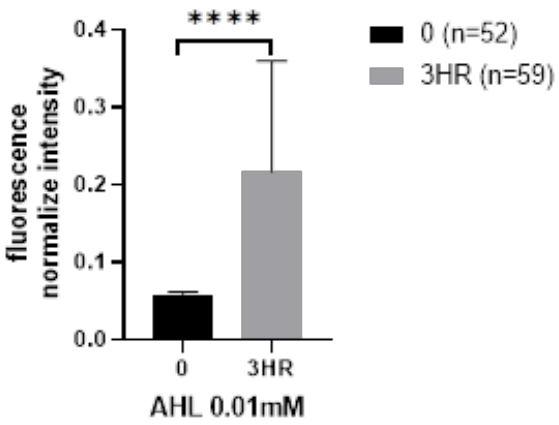

Figure 17. The expression of the anemone Par3 in E. *coli.* (A) The construct diagrams. (B) The fluorescence microscopy images of pLux-his-mRFP-Par3 (anemone). Induce by 0.01mM AHL and incubate at 37℃ for 3 hours.

doi:10.6342/NTU202203638

(C) Fluorescence intensity (mRFP) profiles along the axis of cell. Before the induction (left image) and induce for 3 hours (right image). The fluorescence intensity normalized by the maximal. Gray lines mean that fluorescence intensity of a cell. The red lines indicate averages. (D) Quantification of the normalize fluorescence intensity The Statistical difference was determined by Student's t-test; **** means that the P value < 0.0001.

doi:10.6342/NTU202203638

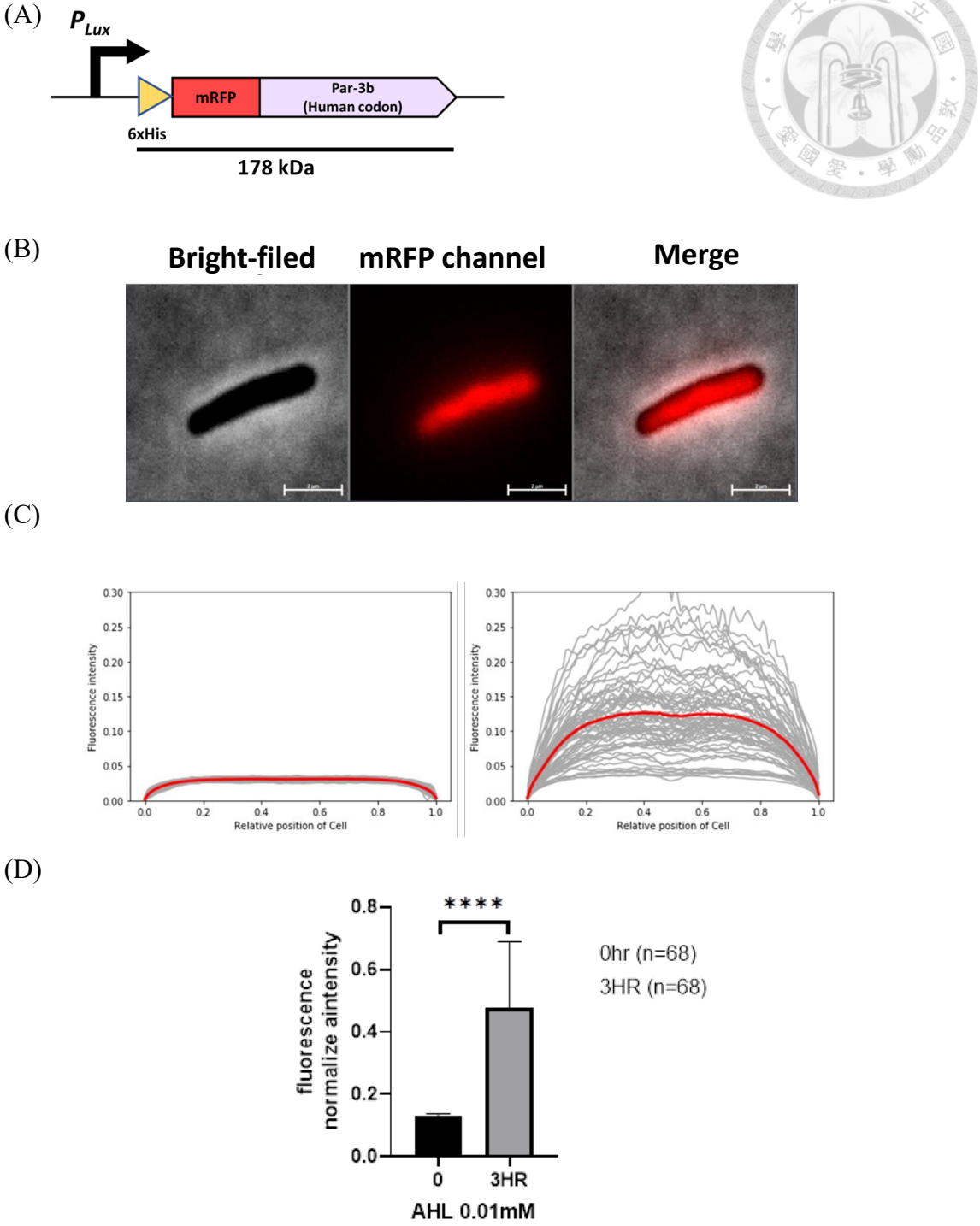

Figure 18. The expression of the human Par3b in E. *coli.* (A) The construct diagrams. (B) The fluorescence microscopy images of pLux-his-mRFP-Par3b (human). Induce by 0.01mM AHL and incubate at 37℃ for 3 hours.

doi:10.6342/NTU202203638

(C) Fluorescence intensity (mRFP) profiles along the axis of cell. Before the induction (left image) and induce for 3 hours (right image). The fluorescence intensity normalized by the maximal. Gray lines mean that fluorescence intensity of a cell. The red lines indicate averages. (D) Quantification of the normalize fluorescence intensity The Statistical difference was determined by Student's t-test; **** means that the P value < 0.0001.

doi:10.6342/NTU202203638

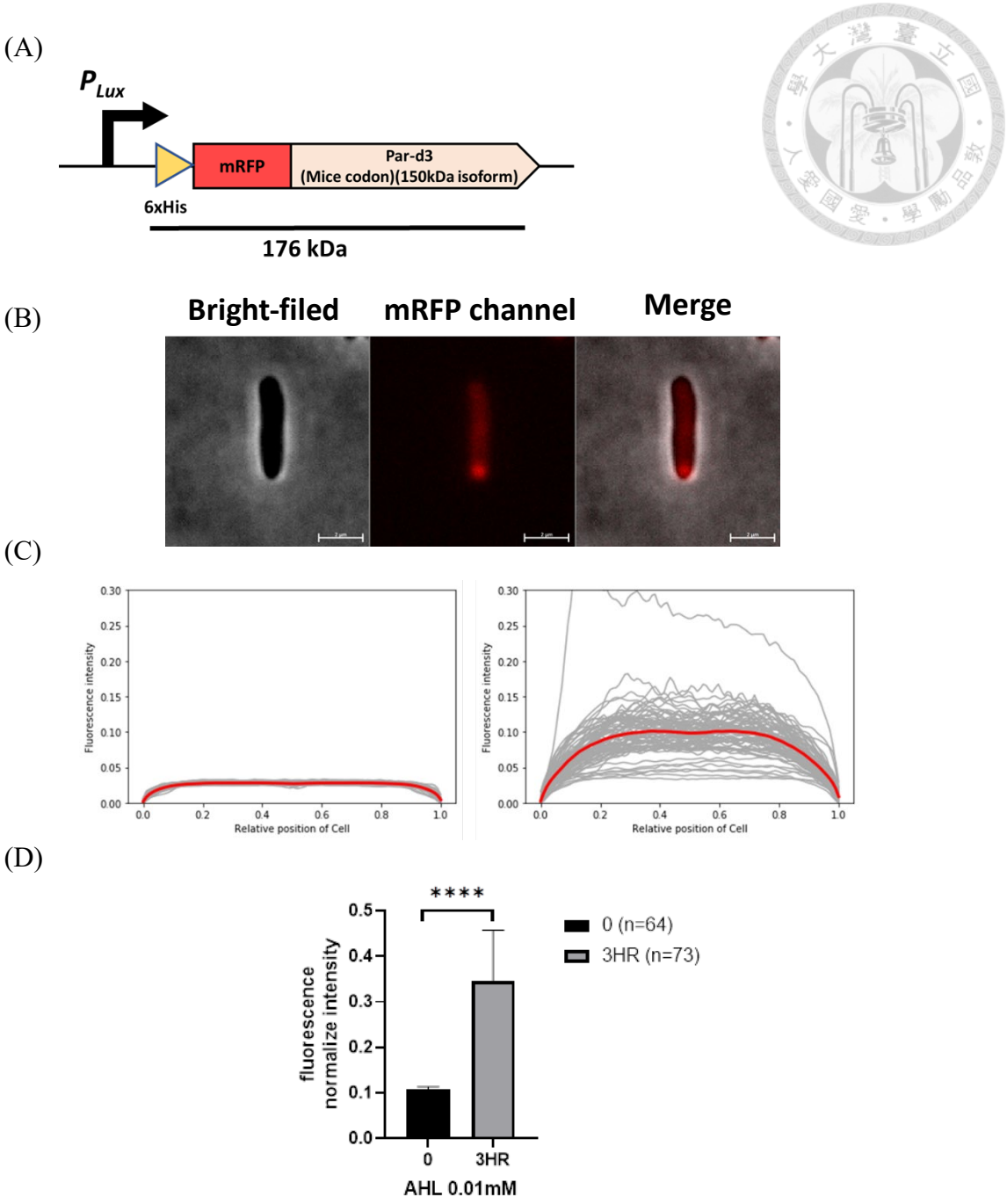

Figure 19. The expression of the Pard3 (mouse) in E. *coli.* (A) The construct diagrams. (B) The fluorescence microscopy images of pLux-his-mRFP-Par3b (human). Induce by 0.01mM AHL and incubate at 37℃ for 3 hours.

doi:10.6342/NTU202203638

(C) Fluorescence intensity (mRFP) profiles along the axis of cell. Before the induction (left image) and induce for 3 hours (right image). The fluorescence intensity normalized by the maximal. Gray lines mean that fluorescence intensity of a cell. The red lines indicate averages. (D) Quantification of the normalize fluorescence intensity The Statistical difference was determined by Student's t-test; **** means that the P value < 0.0001.

doi:10.6342/NTU202203638

(A)

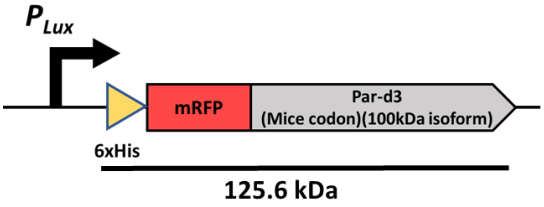

(B)

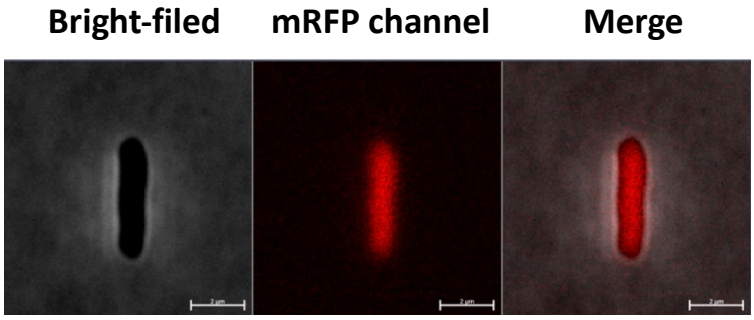

(C)

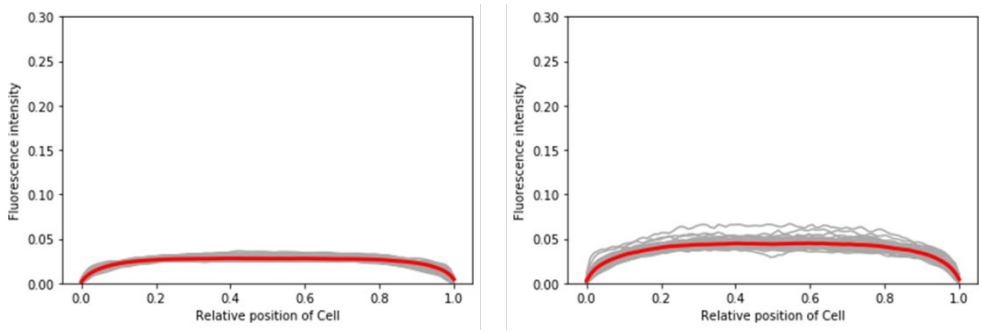

(D)

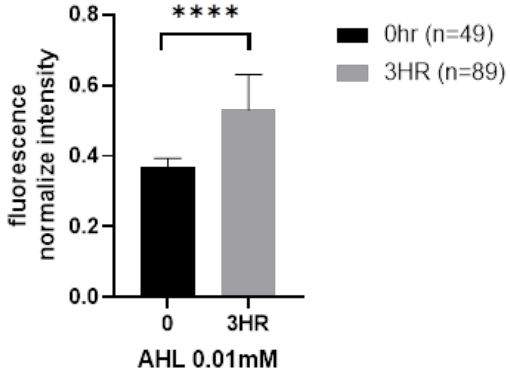

Figure 20. The expression of the mice Pard3 (100kDa isoform) in E. *coli.* (A) The construct diagrams. (B) The fluorescence microscopy images of pLux-his-mRFP-Par3b (mice (100kDa isoform)). Induce by 0.01mM AHL and incubate at 37℃ for 3 hours.

doi:10.6342/NTU202203638

(C) Fluorescence intensity (mRFP) profiles along the axis of cell. Before the induction (left image) and induce for 3 hours (right image). The fluorescence intensity normalized by the maximal. Gray lines mean that fluorescence intensity of a cell. The red lines indicate averages. (D) Quantification of the normalize fluorescence intensity The Statistical difference was determined by Student's t-test; **** means that the P value < 0.0001.

doi:10.6342/NTU202203638

(A)

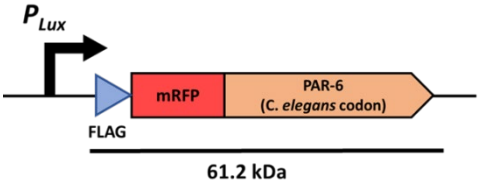

(B)

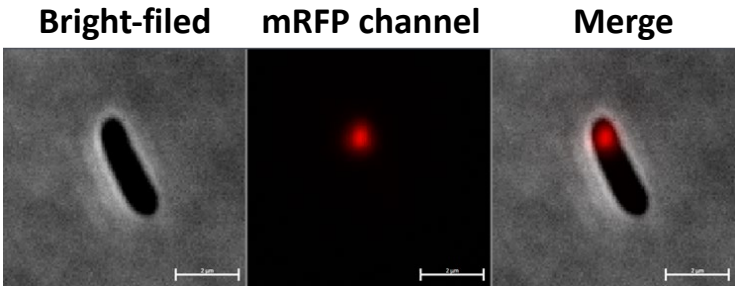

(C)

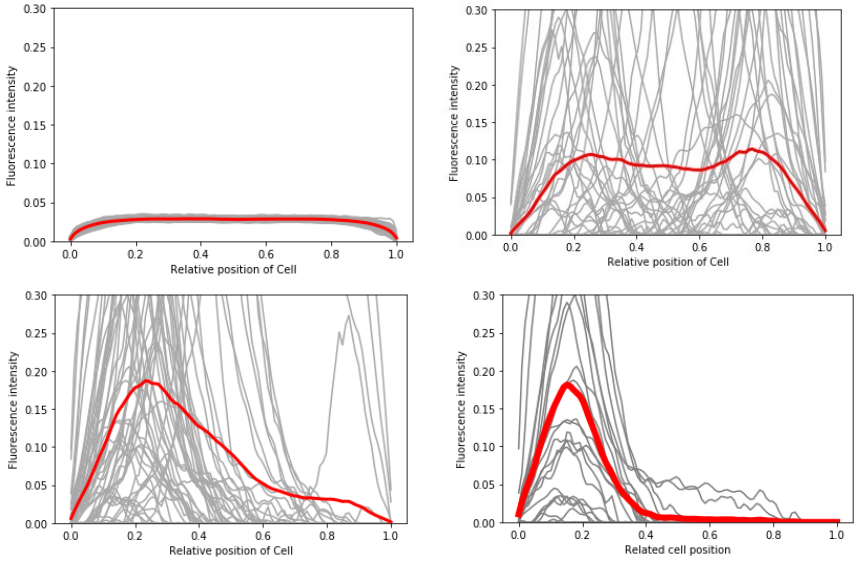

(D)

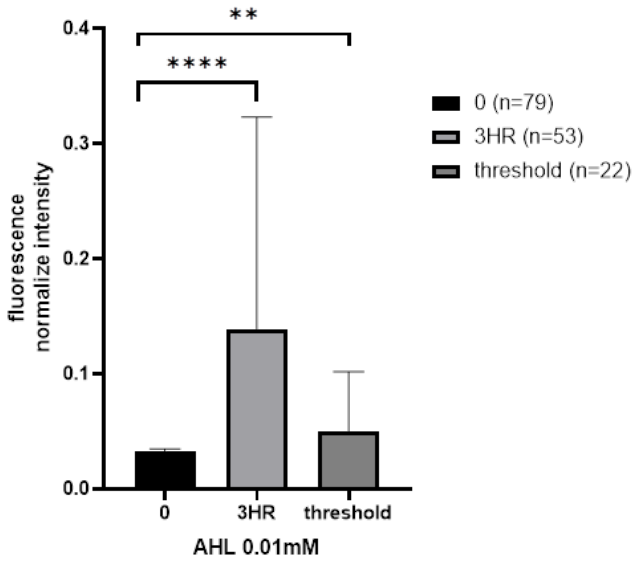

doi:10.6342/NTU202203638

Figure 21. The expression of the C. *elegans* Par-6 in E. *coli*. (A) The construct diagrams. (B) The fluorescence microscopy images of pLux-FLAG-mRFP-Par6 (C. *elegans*). Induce by 0.01mM AHL and incubate at 37℃ for 3 hours. (C) Fluorescence intensity (mRFP) profiles along the axis of cell. Before the induction (top left image) and induce for 3 hours (top right image). The intensity is flipped to the same side (bottom left image). And the fluorescence intensity data analysis by Otsu's thresholding method (bottom right image). The fluorescence intensity normalized by the maximal. Gray lines mean that fluorescence intensity of a cell. The red lines indicate averages. (D) Quantification of the normalize fluorescence intensity The Statistical difference was determined by Student's t-test; **** means that the P value < 0.0001.

doi:10.6342/NTU202203638

(A)

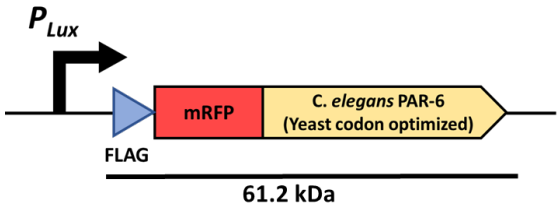

(B)

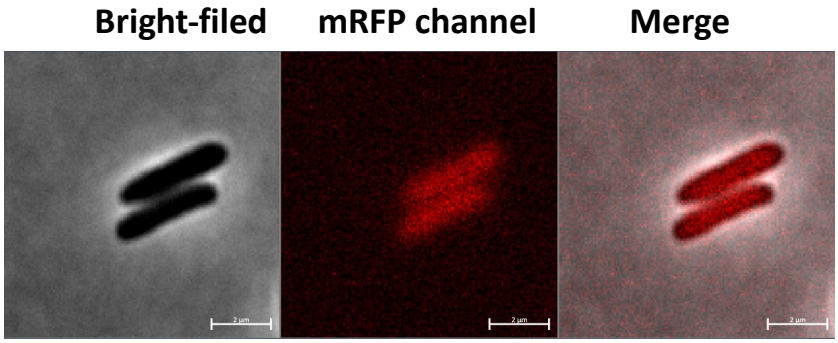

(C)

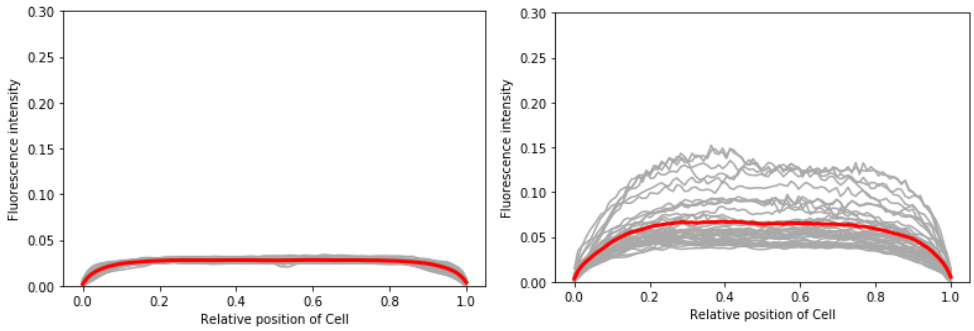

(D)

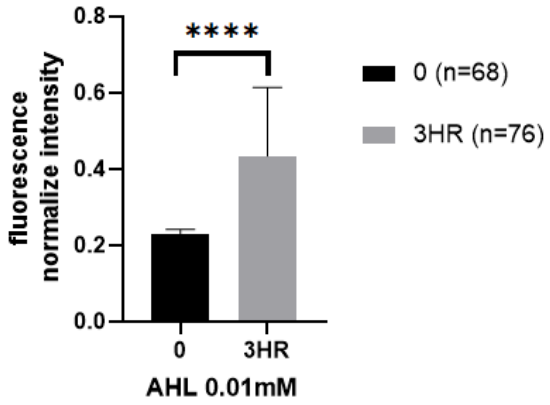

Figure 22. The expression of the C. *elegans* Par-6 (yeast codon) in E. *coli*. (A) The construct diagrams. (B) The fluorescence microscopy images of pLux-FLAG-mRFP-Par6 (yeast codon). Induce by 0.01mM AHL and incubate at 37℃ for 3 hours.

doi:10.6342/NTU202203638

(C) Fluorescence intensity (mRFP) profiles along the axis of cell. Before the induction (left image) and induce for 3 hours (right image). The fluorescence intensity normalized by the maximal. Gray lines mean that fluorescence intensity of a cell. The red lines indicate averages. (D) Quantification of the normalize fluorescence intensity The Statistical difference was determined by Student's t-test; **** means that the P value < 0.0001.

doi:10.6342/NTU202203638

(A)

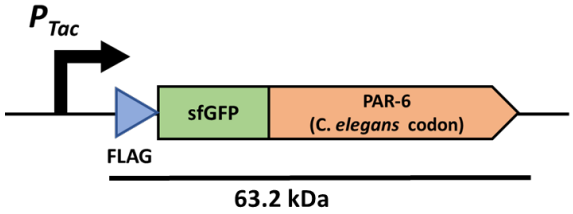

(B)

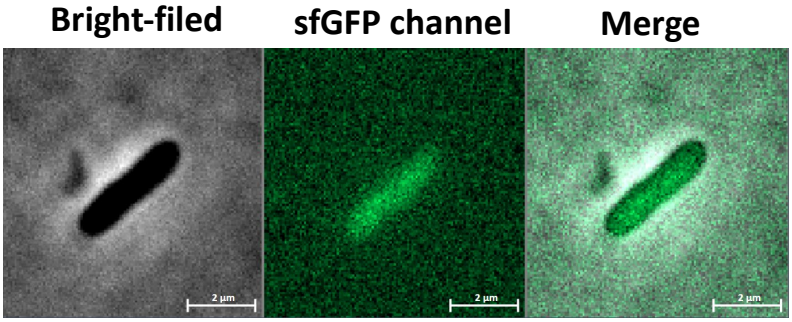

(C)

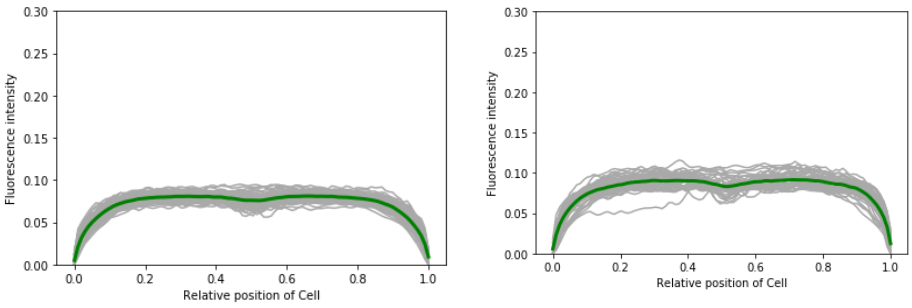

(D)

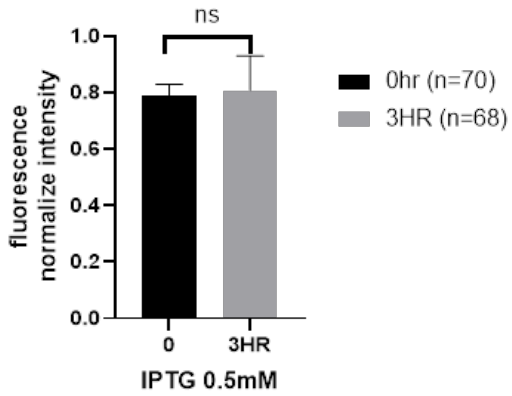

Figure 23. The expression of the Par-6 (C. *elegans*) driven by pTac promoter in E. *coli*. (A) The construct diagrams. (B) The fluorescence microscopy images of pTac-FLAG-sfGFP-Par6 (C. *elegans*). Induce by 0.5mM IPTG and incubate at 37℃ for 3 hours.

doi:10.6342/NTU202203638

(C) Fluorescence intensity (sfGFP) profiles along the axis of cell. Before the induction (left image) and induce for 3 hours (right image). The fluorescence intensity normalized by the maximal. Gray lines mean that fluorescence intensity of a cell. The green lines indicate averages. (D) Quantification of the normalize fluorescence intensity. The Statistical difference was determined by Student's t-test; P value = 0.24. No significantly different.

doi:10.6342/NTU202203638

(A)

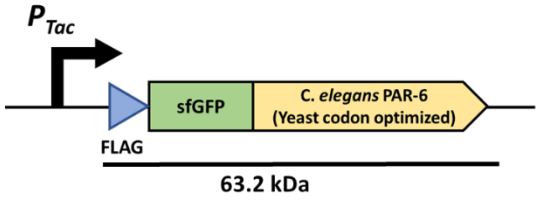

(B)

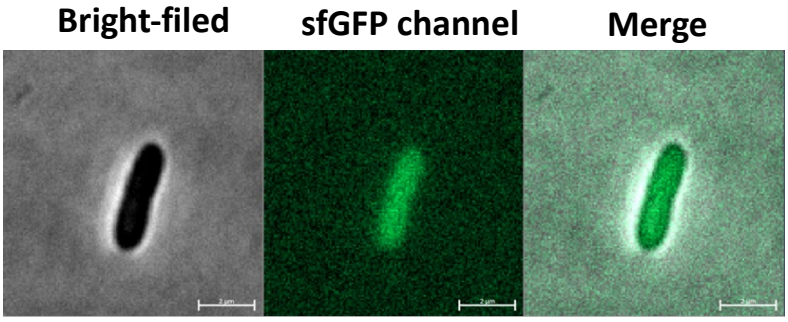

(C)

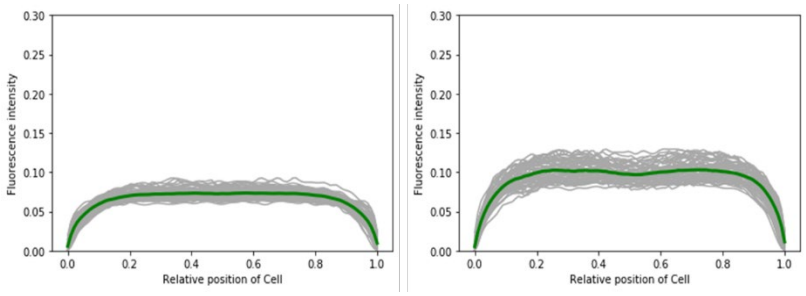

(D)

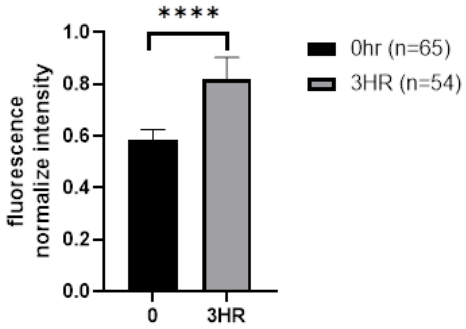

Figure 24. The expression of the Par-6 (C. *elegans* cDNAs with yeast optimized) in E. *coli*. (A) The construct diagrams. (B) The fluorescence microscopy images of pTac-FLAG-sfGFP-Par6 (C. *elegans* cDNAs with yeast optimized). Induce by 0.5mM IPTG and incubate at 37℃ for 3 hours.

doi:10.6342/NTU202203638

(C) Fluorescence intensity (sfGFP) profiles along the axis of cell. Before the induction (left image) and induce for 3 hours (right image). The fluorescence intensity normalized by the maximal. Gray lines mean that fluorescence intensity of a cell. The green lines indicate averages. (D) Quantification of the normalize fluorescence intensity. The Statistical difference was determined by Student's t-test; **** means that the P value < 0.0001.

doi:10.6342/NTU202203638

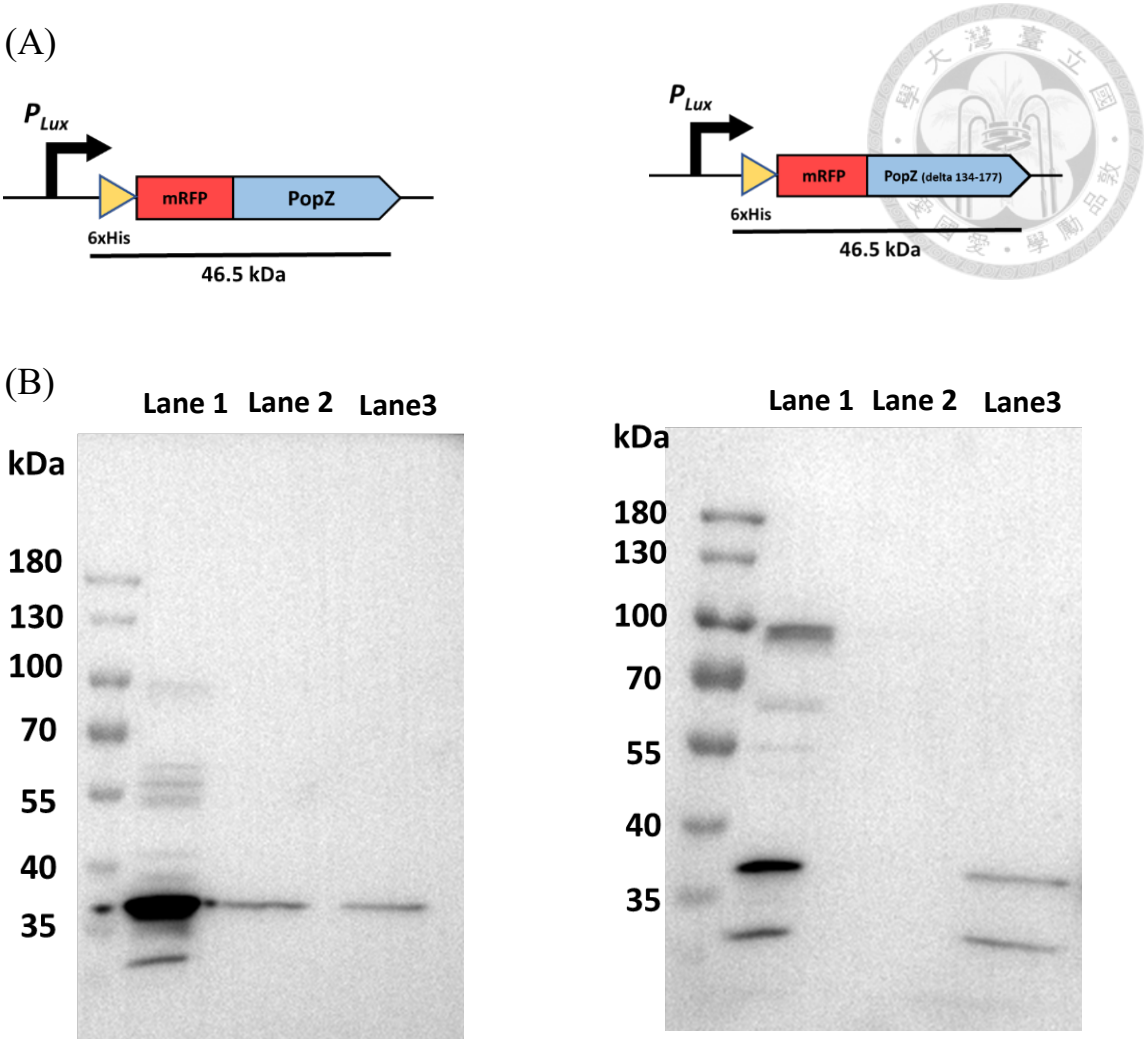

Figure 25. (A) The construct diagrams and the predicted molecular weight. (B) Induced by 0.01mM AHL for 6 hours at 37℃. The E. *coli* lysate (lane 1) purified by his-tagged protein isolation & pulldown (lane 2 and lane 3, lane 2 was elution buffer 1 and lane 3 was elution buffer 2) and separated by SDS-PAGE electrophoresis, with molecular weight standards (in kDa) in the left-most lane. The gels were analyzed by Western blotting with anti-His tag antibody (1:5000).

doi:10.6342/NTU202203638

(A)

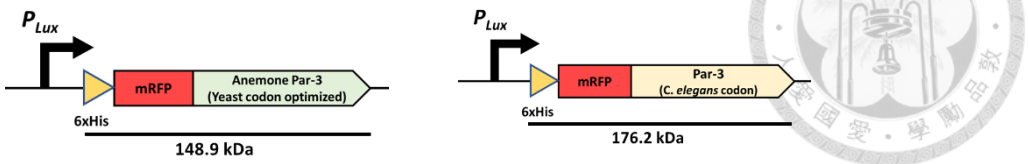

(B)

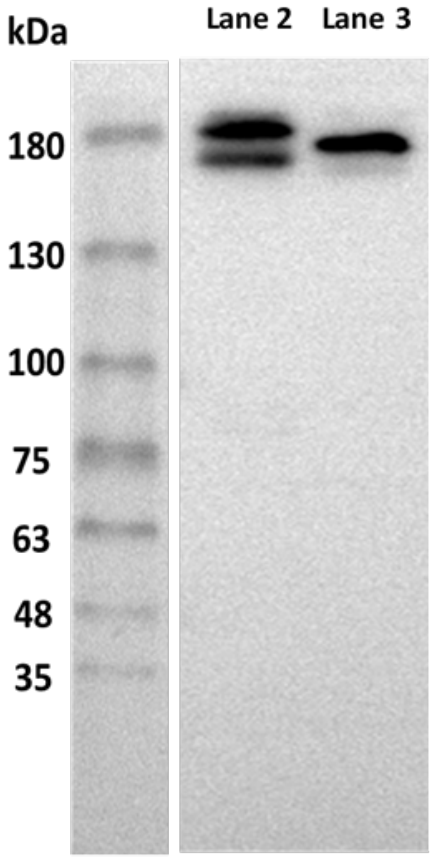

Figure 26. (A) The construct diagrams and the predicted molecular weight. (B) Induced by 0.01mM AHL for 6 hours at 37℃. The E. *coli* lysate separated by SDS-PAGE electrophoresis, with molecular weight standards (in kDa) in the left-most lane. The gels were analyzed by Western blotting with anti-His tag antibody (1:5000).

doi:10.6342/NTU202203638

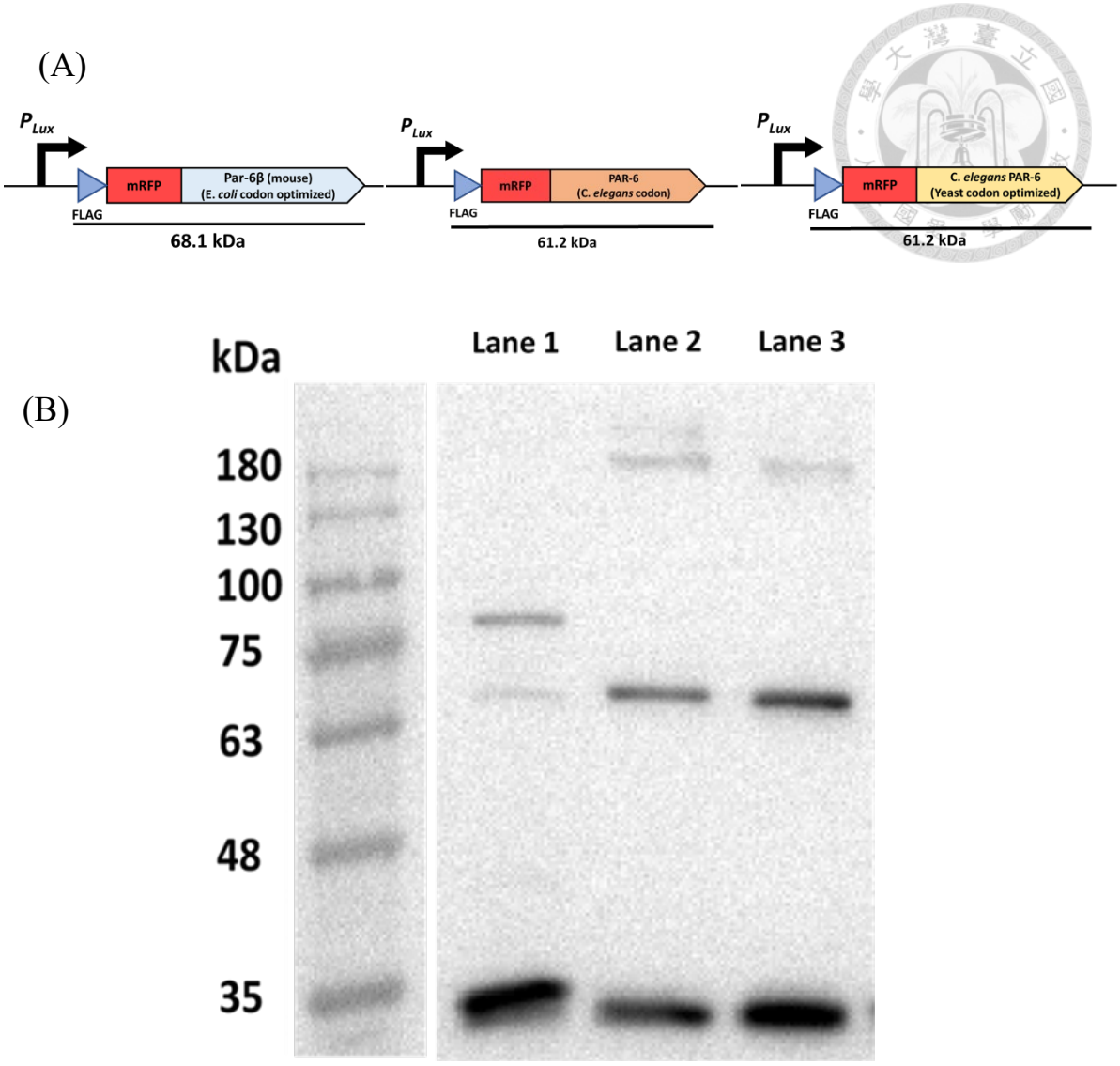

Figure 27. (A) The construct diagrams and the predicted molecular weight. (B) Induced by 0.01mM AHL for 6 hours at 37℃. The E. *coli* lysate separated by SDS-PAGE electrophoresis, with molecular weight standards (in kDa) in the left-most lane. The gels were analyzed by Western blotting with anti-FLAG antibody (1:5000).

doi:10.6342/NTU202203638

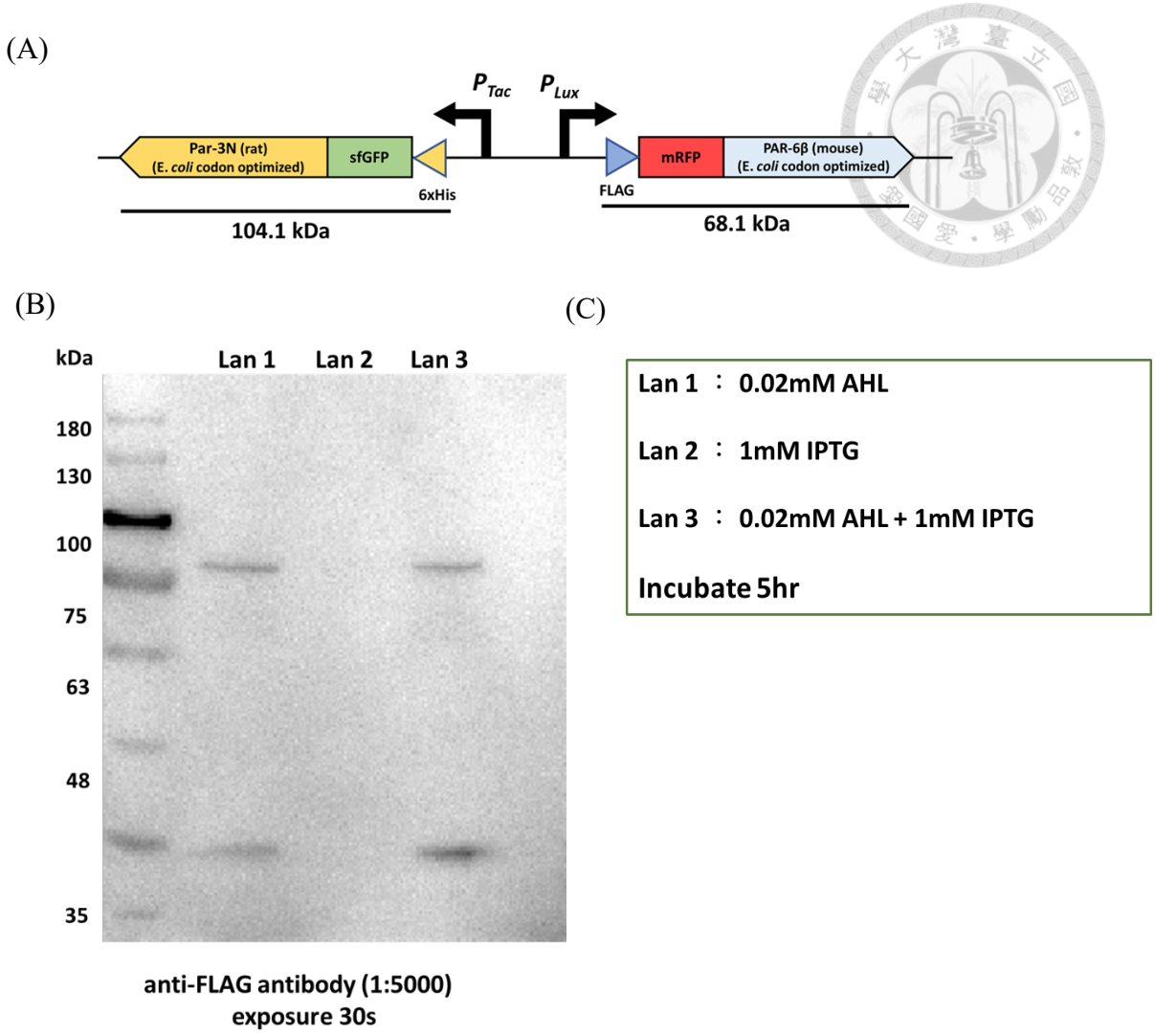

Figure 28. (A) The construct diagrams. (B) Co-Immunoprecipitation (Co-IP) experiments. The E. *coli* lysate purified by his-tagged protein isolation & pulldown and separated by SDS-PAGE electrophoresis, with molecular weight standards (in kDa) in the left-most lane. The gels were analyzed by Western blotting with anti-FLAG antibody. (C) The induction condition of the samples. These three groups were under the same experimental environment and conditions, subculture, induction and harvesting centrifugation were carried out at the same time.

doi:10.6342/NTU202203638

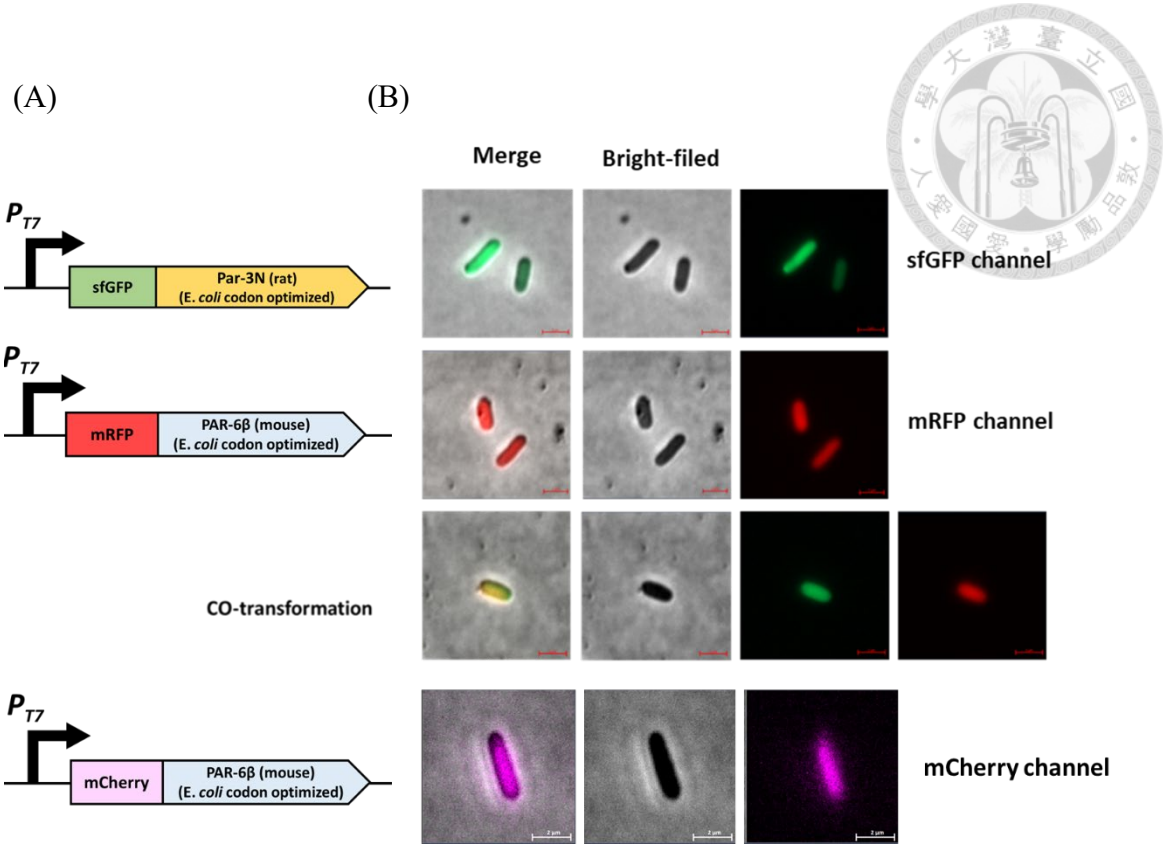

Figure 29. The expression of the Par3N and Par6β in BLR (DE3) by T7 promoter. (A) The construct diagrams. (B) The fluorescence microscopy images of pT7-mRFP-Par3N, pT7- mRFP-Par6β and pT7- mCherry-Par6β. Induce by 0.5mM IPTG and incubate at 37℃ for 3 hours.

doi:10.6342/NTU202203638

(A)

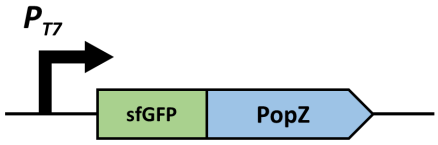

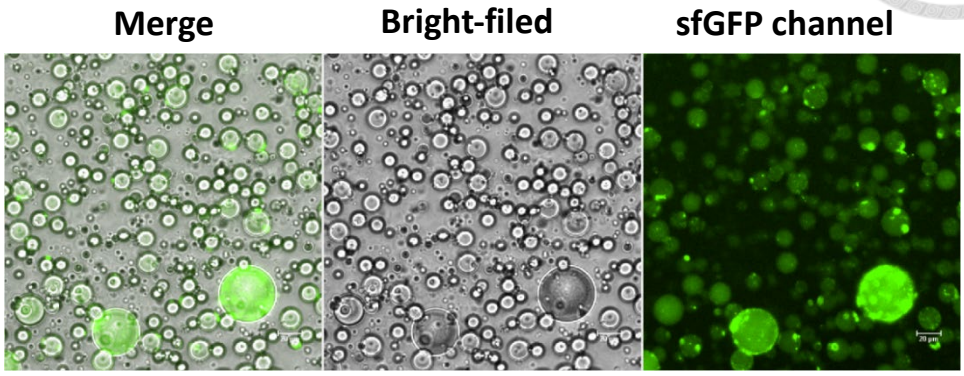

(B)

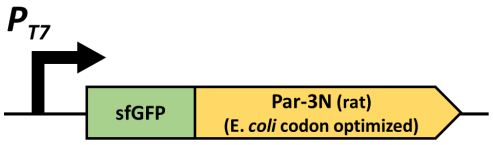

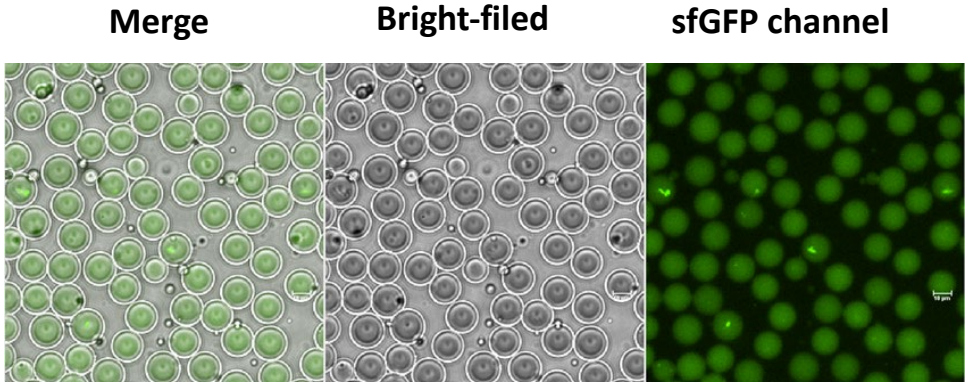

(C)

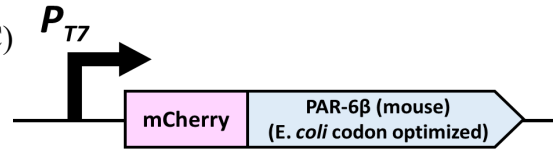

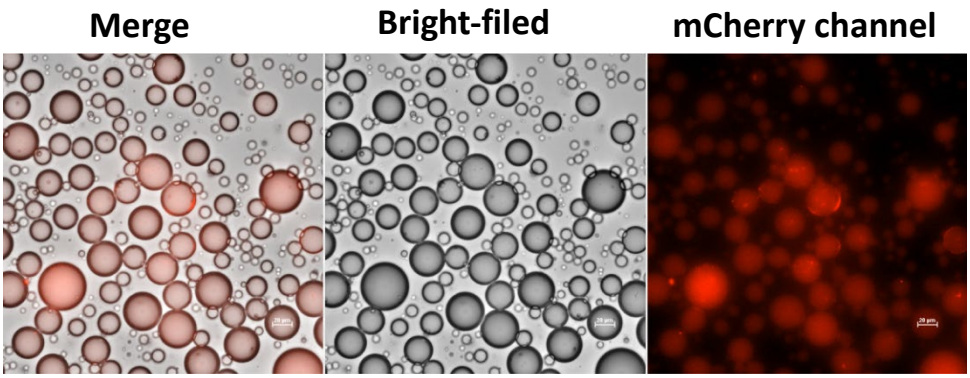

doi:10.6342/NTU202203638

(D)

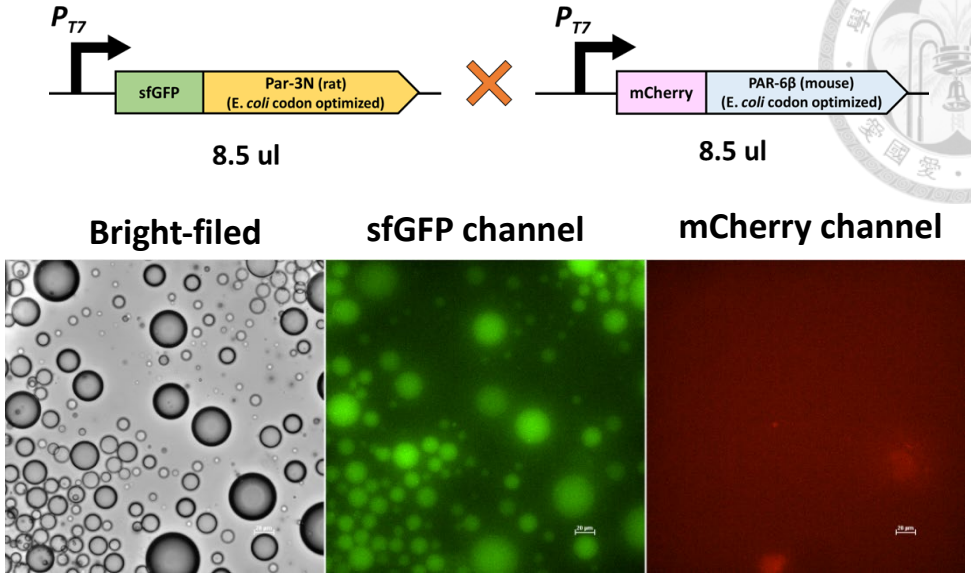

Figure 30. The expression of the Par3N and Par6β in droplet by IVTT for 3 hours. (A) The fluorescence microscopy images of pT7-sfGFP-popZ, the positive control. (B) The fluorescence microscopy images of pT7-sfGFP-par3N. (C) The fluorescence microscopy images of T7-mCherry-par6β. (D) The fluorescence microscopy images of pT7-sfGFP-par3N + pT7-mCherry-par6β.

doi:10.6342/NTU202203638

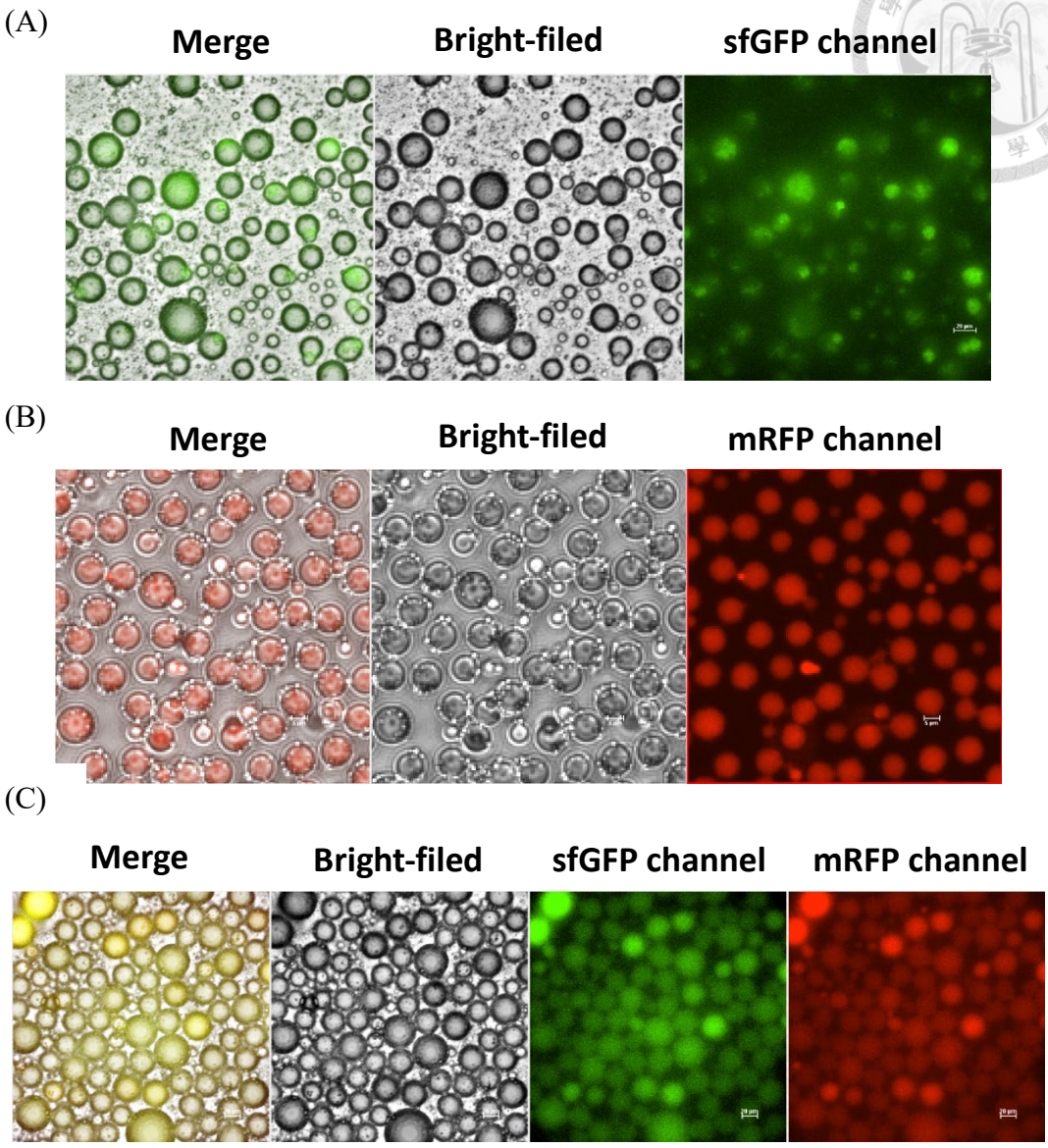

Figure 31. The expression of the Par3N and Par6β in droplet by cell lysis. (A) The fluorescence microscopy images of pTac-histag-sfGFP-par3N cell lysate. (B) The fluorescence microscopy images of pLux-FLAG-mRFP-Par6β cell lysate. (C) The fluorescence microscopy images of pLux-FLAG-mRFP-Par6β_pTac-his-sfGFP-par3N(r) cell lysate.

doi:10.6342/NTU202203638

6. Reference

Abil, Z., Xiong, X., & Zhao, H. (2015). Synthetic Biology for Therapeutic Applications. *Molecular Pharmaceutics, 12*(2), 322-331. doi:10.1021/mp500392q

Belahbib, H., Renard, E., Santini, S., Jourda, C., Claverie, J.-M., Borchiellini, C., & Le Bivic, A. (2018). New genomic data and analyses challenge the traditional vision of animal epithelium evolution. *BMC Genomics, 19*(1). doi:10.1186/s12864-018-4715-9

Benner, S. A., & Sismour, A. M. (2005). Synthetic biology. *Nature Reviews Genetics, 6*(7), 533-543. doi:10.1038/nrg1637

Fahey, B., & Degnan, B. M. (2010). Origin of animal epithelia: insights from the sponge genome. *Evolution & Development, 12*(6), 601-617. doi:10.1111/j.1525-142x.2010.00445.x

Feng, W., Wu, H., Chan, L.-N., & Zhang, M. (2007). The Par-3 NTD adopts a PB1-like structure required for Par-3 oligomerization and membrane localization. *The EMBO Journal, 26*(11), 2786-2796. doi:10.1038/sj.emboj.7601702

Heng, B. C., & Fussenegger, M. (2013). Chapter 9 - Design and Application of Synthetic Biology Devices for Therapy. In H. Zhao (Ed.), *Synthetic Biology* (pp. 159-181). Boston: Academic Press.

Holmes, J. A., Follett, S. E., Wang, H., Meadows, C. P., Varga, K., & Bowman, G. R. (2016). Caulobacter PopZ forms an intrinsically disordered hub in organizing bacterial cell poles. *Proceedings of the National Academy of Sciences, 113*(44), 12490-12495. doi:10.1073/pnas.1602380113

Hwang, S. Y., & Rose, L. S. (2010). Control of asymmetric cell division in early C. elegans embryogenesis: teaming-up translational repression and protein degradation. *BMB reports, 43 2*, 69-78.

Ikeshima-Kataoka, H., Skeath, J. B., Nabeshima, Y.-i., Doe, C. Q., & Matsuzaki, F. (1997). Miranda directs Prospero to a daughter cell during Drosophila asymmetric divisions. *Nature, 390*(6660), 625-629. doi:10.1038/37641

Jacob, F., & Monod, J. (1961). Genetic regulatory mechanisms in the synthesis of proteins. *Journal of Molecular Biology, 3*(3), 318-356. doi:https://doi.org/10.1016/S0022-2836(61)80072-7

Kemphues, K. J., Priess, J. R., Morton, D. G., & Cheng, N. (1988). Identification of genes required for cytoplasmic localization in early C. elegans embryos. *Cell, 52*(3), 311-320. doi:https://doi.org/10.1016/S0092-8674(88)80024-2

Liu, Z., Yang, Y., Gu, A., Xu, J., Mao, Y., Lu, H., . . . Wen, W. (2020). Par complex cluster formation mediated by phase separation. *Nature Communications,*

doi:10.6342/NTU202203638

11(1). doi:10.1038/s41467-020-16135-6

Mushnikov, N. V., Fomicheva, A., Gomelsky, M., & Bowman, G. R. (2019). Inducible asymmetric cell division and cell differentiation in a bacterium. *Nature Chemical Biology, 15*(9), 925-931. doi:10.1038/s41589-019-0340-4

Neumüller, R. A., & Knoblich, J. A. (2009). Dividing cellular asymmetry: asymmetric cell division and its implications for stem cells and cancer. *Genes & Development, 23*(23), 2675-2699. doi:10.1101/gad.1850809

Paintdakhi, A., Parry, B., Campos, M., Irnov, I., Elf, J., Surovtsev, I., & Jacobs-Wagner, C. (2016). Oufti: an integrated software package for high-accuracy, high-throughput quantitative microscopy analysis. *Molecular Microbiology, 99*(4), 767-777. doi:10.1111/mmi.13264

Petronczki, M., & Knoblich, J. A. (2001). DmPAR-6 directs epithelial polarity and asymmetric cell division of neuroblasts in Drosophila. *Nature Cell Biology, 3*(1), 43-49. doi:10.1038/35050550

Purnick, P. E. M., & Weiss, R. (2009). The second wave of synthetic biology: from modules to systems. *Nature Reviews Molecular Cell Biology, 10*(6), 410-422. doi:10.1038/nrm2698

Renschler, F. A., Bruekner, S. R., Salomon, P. L., Mukherjee, A., Kullmann, L., Schütz-Stoffregen, M. C., . . . Wiesner, S. (2018). Structural basis for the interaction between the cell polarity proteins Par3 and Par6. *Sci Signal, 11*(517). doi:10.1126/scisignal.aam9899

Renschler, F. A., Bruekner, S. R., Salomon, P. L., Mukherjee, A., Kullmann, L., Schütz-Stoffregen, M. C., . . . Wiesner, S. (2018). Structural basis for the interaction between the cell polarity proteins Par3 and Par6. *Science Signaling, 11*(517), eaam9899. doi:doi:10.1126/scisignal.aam9899

Saha, S., Weber, C. A., Nousch, M., Adame-Arana, O., Hoege, C., Hein, M. Y., . . . Hyman, A. A. (2016). Polar Positioning of Phase-Separated Liquid Compartments in Cells Regulated by an mRNA Competition Mechanism. *Cell, 166*(6), 1572-1584.e1516. doi:https://doi.org/10.1016/j.cell.2016.08.006

Salinas-Saavedra, M., Stephenson, T. Q., Dunn, C. W., & Martindale, M. Q. (2015). Par system components are asymmetrically localized in ectodermal epithelia, but not during early development in the sea anemone Nematostella vectensis. *EvoDevo, 6*(1), 20. doi:10.1186/s13227-015-0014-6

Schweisguth, F. (2015). Asymmetric cell division in the Drosophila bristle lineage: from the polarization of sensory organ precursor cells to Notch-mediated binary fate decision. *WIREs Developmental Biology, 4*(3), 299-309. doi:10.1002/wdev.175

Thompson, B. J. (2022). Par-3 family proteins in cell polarity & adhesion. *The*

doi:10.6342/NTU202203638

FEBS Journal, 289(3), 596-613. doi:10.1111/febs.15754

Ting, Z., & Chengyuan, L. *Journal of Advanced Computational Intelligence and Intelligent Informatics VL - 21 IS - 2 SP - 247 EP - 250 PY - 2017 DO - 10.20965/jaciii.2017.p0247 ER -*.

Vinot, S., Le, T., Ohno, S., Pawson, T., Maro, B., & Louvet-Vallée, S. (2005). Asymmetric distribution of PAR proteins in the mouse embryo begins at the 8-cell stage during compaction. *Dev Biol, 282*(2), 307-319. doi:10.1016/j.ydbio.2005.03.001

Wang, B., Zhang, L., Dai, T., Qin, Z., Lu, H., Zhang, L., & Zhou, F. (2021). Liquid–liquid phase separation in human health and diseases. *Signal Transduction and Targeted Therapy, 6*(1), 290. doi:10.1038/s41392-021-00678-1

Westerhoff, H. V., & Palsson, B. O. (2004). The evolution of molecular biology into systems biology. *Nature Biotechnology, 22*(10), 1249-1252. doi:10.1038/nbt1020

Wu, H., Feng, W., Chen, J., Chan, L.-N., Huang, S., & Zhang, M. (2007). PDZ Domains of Par-3 as Potential Phosphoinositide Signaling Integrators. *Molecular Cell, 28*(5), 886-898. doi:https://doi.org/10.1016/j.molcel.2007.10.028

Xu, X., Xu, S., Jin, L., & Song, E. (2011). Characteristic analysis of Otsu threshold and its applications. *Pattern Recognition Letters, 32*(7), 956-961. doi:https://doi.org/10.1016/j.patrec.2011.01.021

Yu, C. G., Tonikian, R., Felsensteiner, C., Jhingree, J. R., Desveaux, D., Sidhu, S. S., & Harris, T. J. C. (2014). Peptide Binding Properties of the Three PDZ Domains of Bazooka (Drosophila Par-3). *PLOS ONE, 9*(1), e86412. doi:10.1371/journal.pone.0086412

doi:10.6342/NTU202203638

Appendix I. The organizations design of the constructs Par-3N and Par-6β

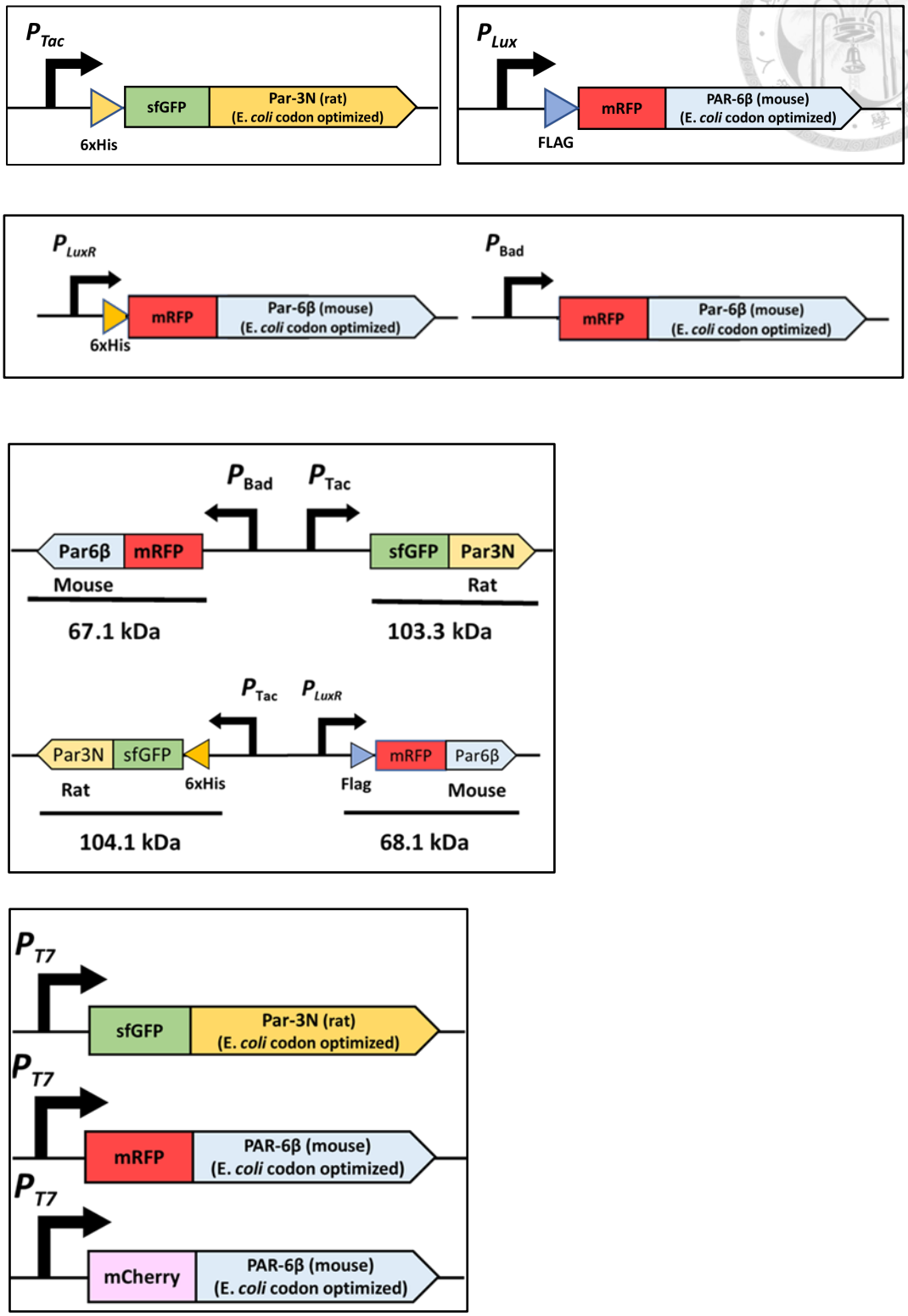

doi:10.6342/NTU202203638

Appendix II. The organizations design of the constructs Par-3 homologous

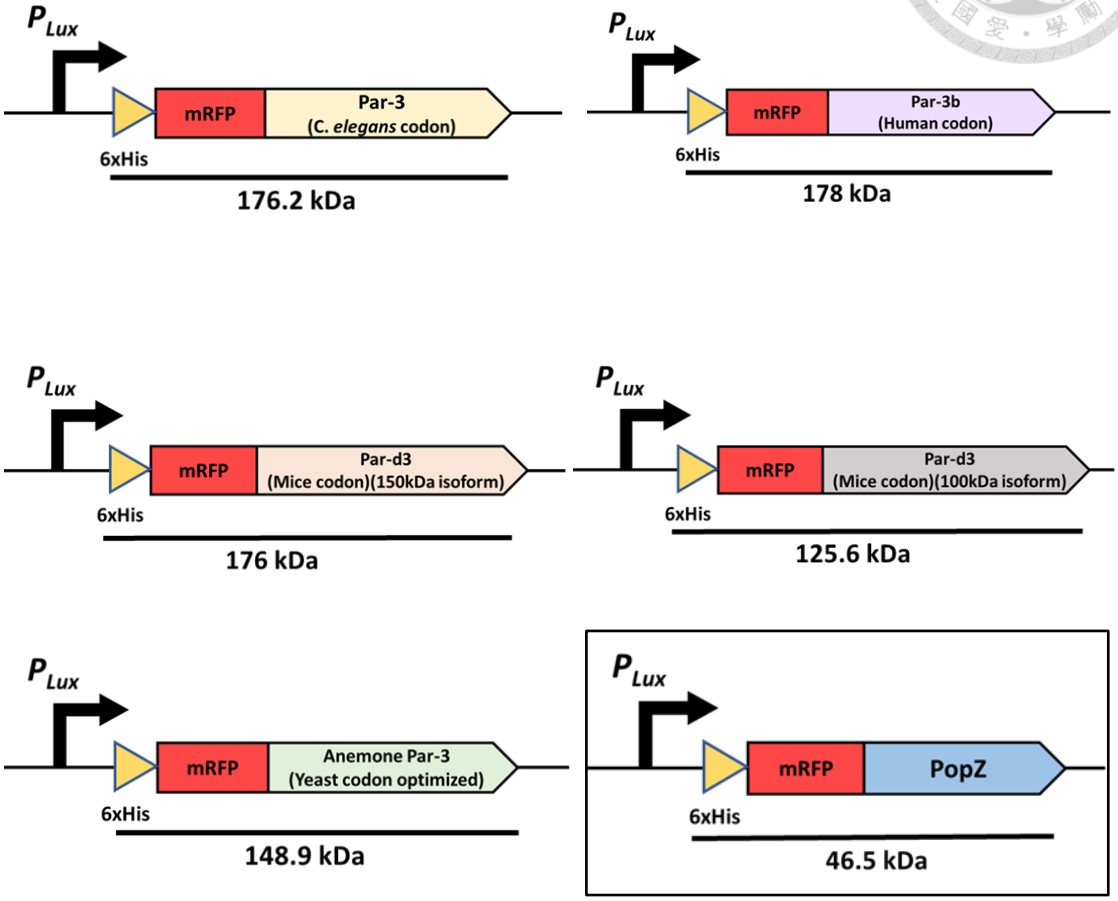

✓ The list of schematic diagrams showing the organizations design of the constructs about Par-3 homologous. And we used PopZ as our positive control.

doi:10.6342/NTU202203638

Appendix III. The organizations design of the constructs Par-6

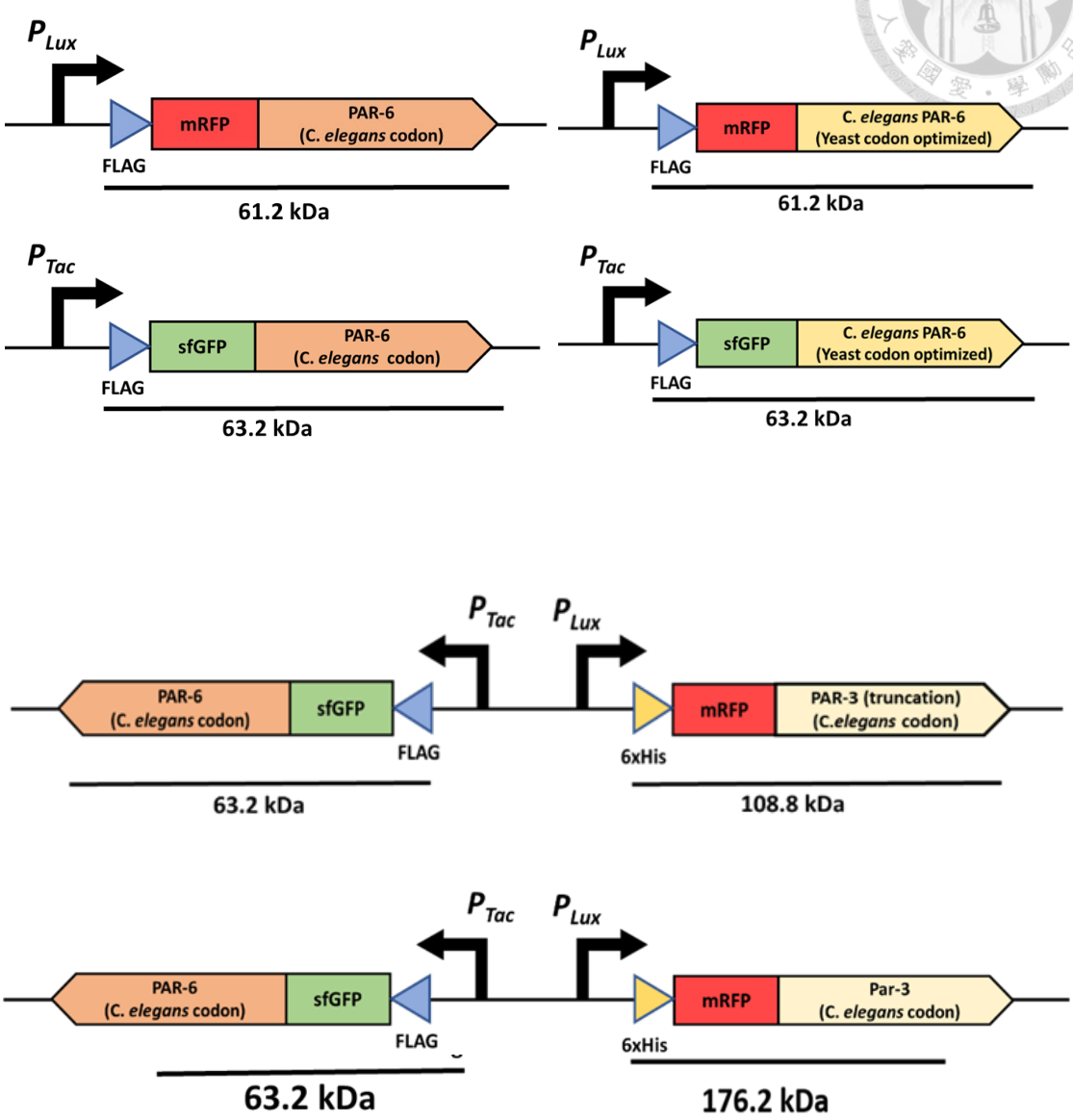

doi:10.6342/NTU202203638

Appendix IV. Conserved domains search result of different species Par3

- The conserved domains of C. *elegans* Par3

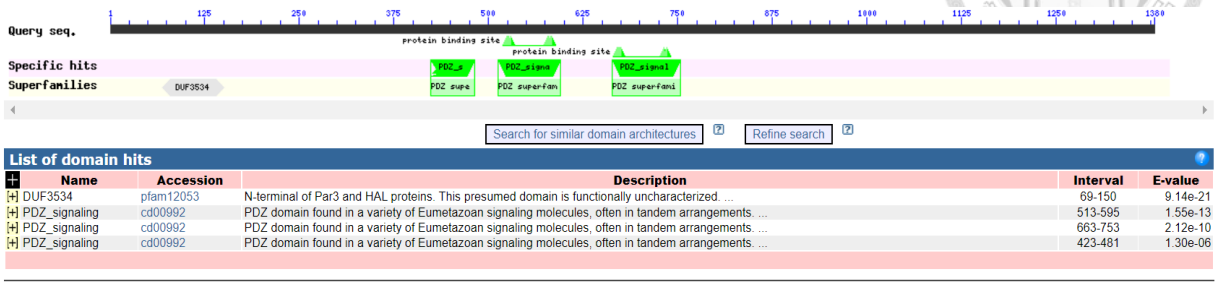

List of domain hits

Name	Accession	Description	Interval	E-value
[+] DUF3534	pfam12053	N-terminal of Par3 and HAL proteins. This presumed domain is functionally uncharacterized. ...	69-150	9.14e-21
[+] PDZ_signaling	cd00992	PDZ domain found in a variety of Eumetazoan signaling molecules, often in tandem arrangements. ...	513-595	1.55e-13
[+] PDZ_signaling	cd00992	PDZ domain found in a variety of Eumetazoan signaling molecules, often in tandem arrangements. ...	663-753	2.12e-10
[+] PDZ_signaling	cd00992	PDZ domain found in a variety of Eumetazoan signaling molecules, often in tandem arrangements. ...	423-481	1.30e-06

- The conserved domains of human Par3b.

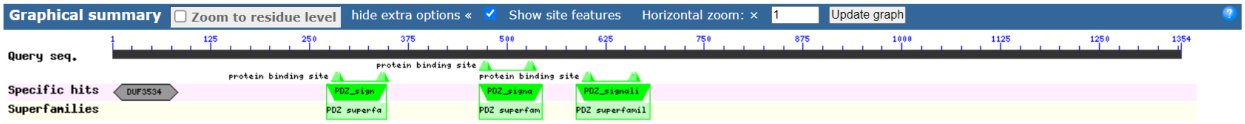

List of domain hits

Name	Accession	Description	Interval	E-value
[+] DUF3534	pfam12053	N-terminal of Par3 and HAL proteins. This presumed domain is functionally uncharacterized. ...	2-83	7.97e-49
[+] PDZ_signaling	cd00992	PDZ domain found in a variety of Eumetazoan signaling molecules, often in tandem arrangements. ...	465-544	3.72e-18
[+] PDZ_signaling	cd00992	PDZ domain found in a variety of Eumetazoan signaling molecules, often in tandem arrangements. ...	588-681	6.37e-16
[+] PDZ_signaling	cd00992	PDZ domain found in a variety of Eumetazoan signaling molecules, often in tandem arrangements. ...	272-347	5.59e-10

- The conserved domains of anemone Par3b.

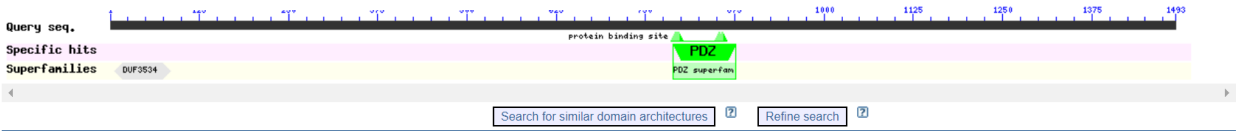

List of domain hits

Name	Accession	Description	Interval	E-value
[+] DUF3534	pfam12053	N-terminal of Par3 and HAL proteins. This presumed domain is functionally uncharacterized. ...	7-84	2.17e-14
[+] PDZ	pfam00595	PDZ domain (Also known as DHR or GLGF); PDZ domains are found in diverse signaling proteins.	788-877	4.35e-14

- The conserved domains of sponge Par3.

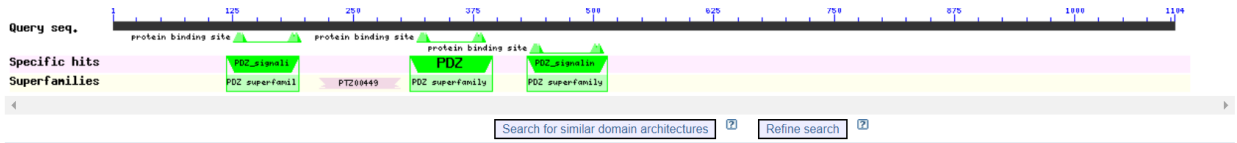

List of domain hits

Name	Accession	Description	Interval	E-value
[+] PDZ	smart00228	Domain present in PSD-95, Dlg, and ZO-1/2; Also called DHR (Dlg homologous region) or GLGF ...	309-395	8.53e-18
[+] PDZ_signaling	cd00992	PDZ domain found in a variety of Eumetazoan signaling molecules, often in tandem arrangements. ...	431-514	1.30e-11
[+] PDZ_signaling	cd00992	PDZ domain found in a variety of Eumetazoan signaling molecules, often in tandem arrangements. ...	118-194	2.05e-10
[+] PTZ00449 super family	cl33186	104 kDa microneme/rhoptry antigen; Provisional	215-299	3.92e-05

doi:10.6342/NTU202203638

➢ The conserved domains of fly Baz.

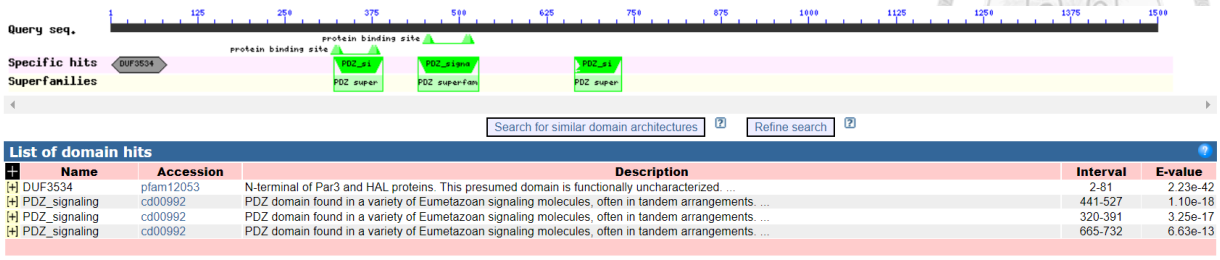

List of domain hits

Name	Accession	Description	Interval	E-value
[+] DUF3534	pfam12053	N-terminal of Par3 and HAL proteins. This presumed domain is functionally uncharacterized. ...	2-81	2.23e-42
[+] PDZ_signaling	cd00992	PDZ domain found in a variety of Eumetazoan signaling molecules, often in tandem arrangements. ...	441-527	1.10e-18
[+] PDZ_signaling	cd00992	PDZ domain found in a variety of Eumetazoan signaling molecules, often in tandem arrangements. ...	320-391	3.25e-17
[+] PDZ_signaling	cd00992	PDZ domain found in a variety of Eumetazoan signaling molecules, often in tandem arrangements. ...	665-732	6.63e-13

➢ The conserved domains of mice Pard3 (150 kDa isoform).

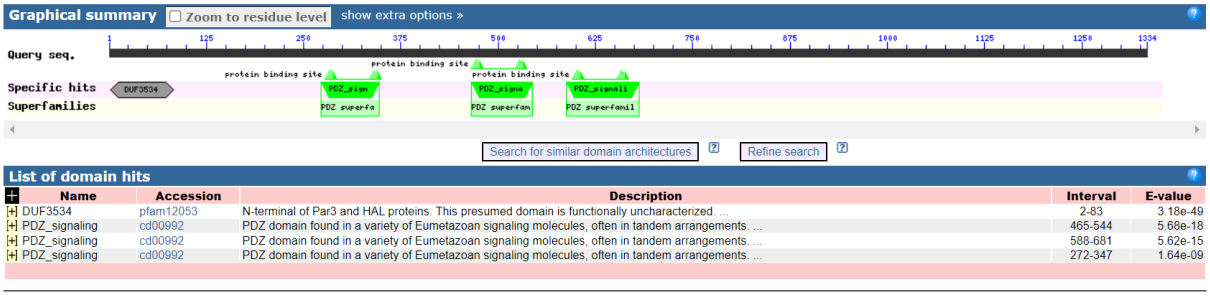

List of domain hits

Name	Accession	Description	Interval	E-value
[+] DUF3534	pfam12053	N-terminal of Par3 and HAL proteins. This presumed domain is functionally uncharacterized. ...	2-83	3.18e-49
[+] PDZ_signaling	cd00992	PDZ domain found in a variety of Eumetazoan signaling molecules, often in tandem arrangements. ...	465-544	5.68e-18
[+] PDZ_signaling	cd00992	PDZ domain found in a variety of Eumetazoan signaling molecules, often in tandem arrangements. ...	588-681	5.62e-15
[+] PDZ_signaling	cd00992	PDZ domain found in a variety of Eumetazoan signaling molecules, often in tandem arrangements. ...	272-347	1.64e-09

➢ The conserved domains of mice Pard3 (100 kDa isoform).

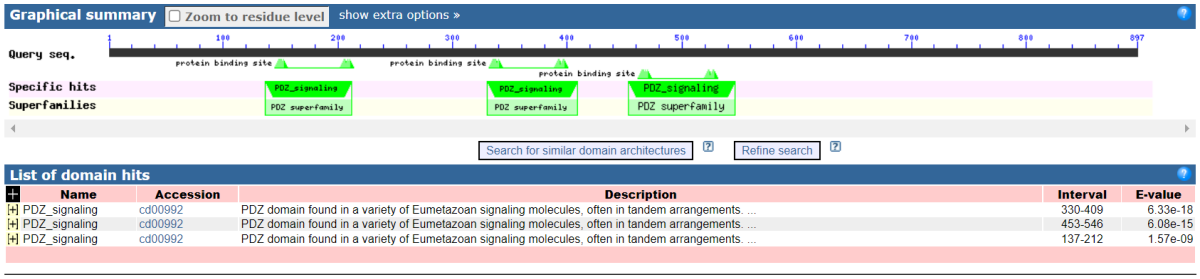

List of domain hits

Name	Accession	Description	Interval	E-value
[+] PDZ_signaling	cd00992	PDZ domain found in a variety of Eumetazoan signaling molecules, often in tandem arrangements. ...	330-409	6.33e-18
[+] PDZ_signaling	cd00992	PDZ domain found in a variety of Eumetazoan signaling molecules, often in tandem arrangements. ...	453-546	6.08e-15
[+] PDZ_signaling	cd00992	PDZ domain found in a variety of Eumetazoan signaling molecules, often in tandem arrangements. ...	137-212	1.57e-09

doi:10.6342/NTU202203638

Appendix V. Python code

```
from scipy import io
import numpy as np
from scipy.stats import pearsonr
import matplotlib.pyplot as plt
import os
from scipy import interpolate
import math

path = "C:/Users/User/Desktop/mat"
os.chdir(path)
files= os.listdir(path)
signal=np.zeros(100)
signal_2=np.zeros(100)
inf = float("inf")
Fluorescence=[]
Fluorescence_2=[]
Pearson_coefficient=[]
Center_mass=[]
Bipolardata=[]
whole_cell_number=[]
for a in range(len(files)):
    mat=io.loadmat(files[a])
    cell_number=mat['cellListN'][0,0]
    whole_cell_number.append(cell_number)

    for i in range(0,cell_number):

        length=len(mat['cellList']['meshData'][0,0][0,0][0,i]['signal1'][0,0])
        x = np.arange(length)
        y=mat['cellList']['meshData'][0,0][0,0][0,i]['signal1'][0,0]
        yi=mat['cellList']['meshData'][0,0][0,0][0,i]['signal2'][0,0]
        if y.shape==(0,0):
            continue
        elif yi.shape==(0,0):
            continue
# ------翻轉----------------------------------------------------------------------
        if np.argmax(y) > length/2:
                y=y[::-1]
                yi=yi[::-1]
```


doi:10.6342/NTU202203638

```
# ------翻轉----------------------------------------------------------------
        if np.argmax(y) > length/2:
                y=y[::-1]
                yi=yi[::-1]
# ------翻轉----------------------------------------------------------------
        if len(y)==1:
            continue
        elif len(yi)==1:
            continue
        y=y[:,0]
        yi=yi[:,0]

#------Total Intensity-----------------------------------------------------
        Fluorescence.append(np.mean(y))
        Fluorescence_2.append(np.mean(yi))
#-------Pearson correlation-------------------------------------------------
        r_row, p_value = pearsonr(y,yi)
        if math.isnan(r_row):
            continue
        Pearson_coefficient.append(r_row)
# #-------Center mass---------------------------------------------------------
        centerdata=np.zeros(length)
        xx=np.linspace(0,1,length)
        for w in range(0,length):
            centerdata[w]=(xx[w]*yi[w])
        if math.isnan(np.sum(centerdata)/np.sum(yi)):
            continue
        Center_mass.append(np.sum(centerdata)/np.sum(yi))
# #-------Unipolar ratio------------------------------------------------------
        bp=max(yi[0:int(length/3)])/max(yi[int(length*2/3):])
        if bp == inf:
            continue
        if math.isnan(bp):
            continue
        Bipolardata.append(bp)
#-------Normalized length---------------------------------------------------
        xnew=np.linspace(x.min(), x.max(),100)
        f=interpolate.interp1d(x,y,'cubic')
        r=interpolate.interp1d(x,yi,'cubic')
        xnewnew=np.linspace(0,1,100)
        ynew=f(xnew)
        ynew2=r(xnew)
        signal=np.column_stack((signal,ynew))
        signal_2=np.column_stack((signal_2,ynew2))

```


doi:10.6342/NTU202203638

```
signal= np.delete(signal,0,1)
signal_2= np.delete(signal_2,0,1)
average=[]
average2=[]
for p in range(0,100):
    average.append(np.mean(signal[p,:]))
for p in range(0,100):
    average2.append(np.mean(signal_2[p,:]))



print('')
plt.xlabel("Relative position of Cell")
plt.ylabel("Fluorescence intensity")
plt.title('Fluorescence sfGFP channel')
plt.ylim(0,0.1)

plt.plot(xnewnew,signal,color='darkgrey')
plt.plot(xnewnew,average,"green",lw=6)

plt.show()

plt.xlabel("Relative position of Cell")
plt.ylabel("Fluorescence intensity")
plt.title('Fluorescence mRFP channel')
plt.ylim(0,0.1)


plt.plot(xnewnew,signal_2,color='darkgrey')
plt.plot(xnewnew,average2,"red",lw=6)
plt.show()


print('Total RFP Intensity:')
print(np.mean(average))
print('')
print('Total GFP Intensity:')
print(np.mean(average2))
print('')
print("Pearson correlation:")
print(np.mean(Pearson_coefficient))
print('')
print('Center mass:')
print(np.mean(Center_mass))
print('')
print('Unipolar degree ratio:')
print(np.mean(Bipolardata))
# print('')
# print('OTSU threshold percentage:')
# print(len(signal[0,:])/np.sum(whole_cell_number)*100,'%')
```


doi:10.6342/NTU202203638